EFFECT OF OXIDATION ON MECHANICAL PROPERTIES OF MODIFIED 9 Cr - 1 Mo STEEL AT HIGH TEMPERATURE

By

MUKESH KUMAR MAHESHWARI

MATERIALS SCIENCE PROGRAMME

INDIAN INSTITUTE OF TECHNOLOGY, KANPUR

MAY, 1984

M.S P- 1984 - M - MAH. EFF

22 AUG 1914

83751

Dedicated

to

Late Mother and Brother

CERTIFICATE

Certified that this work entitled, "Effect of Oxidation on Mechanical Properties of Modified 9Cr-1Mo Steel at High Temperature" has been carried out by Mr.Mukesh Kumar Maheshwari under our supervision and the same has not been submitted elsewhere for a degree

(K N.Rai)
Assistant Professor
Materials Science Programme
Indian Institute of Technology
Kanpur

(K P Singh)
Professor
Dept of Metallurgical Engg.
Indian Institute of Technology
Kanpur

May, 1984.

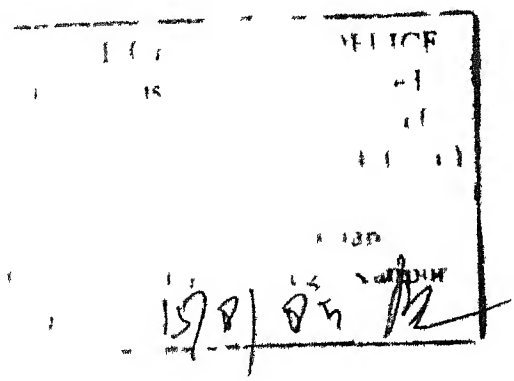

ACKNOWLEDGEMENTS

I feel great pleasure in expressing a profound sense of gratitude to Prof K P Singh and Dr K N Rai for their guidance, cooperation, encouragement throughout the work

I am grateful to Dr R C Sharma, Dr M L Vaidya and Dr S P Gupta for their valuable suggestions and discussions at the various stages of this investigation

I wish to express sincere thanks to Mr M N.Mungole for his unfailing help at every stage of this work.

I take this opportunity to thank Mr K S Bhaumra, Mr Malhotra, Mr B K Jain, Mr V.P Sharma, Mr Sairam, Mr Harishankar for their assistance in time.

I also thank Dr R P Singh and Dr (Mrs) K Khosla who helped during this work

Thanks are due to Messrs S K Tiwari, D K Rawat, Jha A Verma, S Swarup, G Shankar, D Basu and other colleagues for their cooperation and inspiration.

I thankfully acknowledge the Department of Atomic Energy for partial financial support

Finally, I appreciate Mr U S Misra for excellent typing

-Mukesh Kumar Maheshwari

CONTENTS

SYNOPSIS

Effect of oxidation on mechanical properties of modified 9Cr-1Mo ferritic steel is studied in the temperature range of 25°C to 540°C with respect to two different type of Heat Treatment, normalized and tempered (1040°C for 1 hr, air cooled to room temperature, 760°C for 1 hr, air cooled to room temperature), annealed and normalized (850°C for 1 hr, furnace cooled to room temperature, 760°C for 1 hr, air cooled to room temperature) Heat treated samples were oxidized at 650°C at one atmospheric pressure of commercial oxygen for varying times in order to get the required oxygen in sample Effect of microstructure on various mechanical properties (tensile, fatigue, creep-fatigue, stress-rupture) has been discussed

Mechanical tested samples were examined using optical microscopy, SEM and X-ray diffraction.

CHAPTER 1

INTRODUCTION

The currently 9-12 Cr ferritic steels are of high-level interest for pressurized components at high temperature, in power generating industries[1-7] A strong recommendation is made for the development of a modified 9 Cr-1 Mo high strength steel to offset the difficulties encountered with commercially available steels of the 8-12% Cr group because of its good corrosion resistance, dimensional stability at higher temperature, weldability, fabricability, void swelling resistance, mechanical properties[1,4-8] Substitution of 9 Cr-1 Mo steel for 18 Cr - 8 Ni steels will constitute significant conservation of both chromium and nickel[2,9,10] Due to these properties, it is being considered for the future structural material in solar central receivers, fossile system, nuclear electric power generating industry, like Liquid Metal Fast Breeder Reactor (LMFBR), Fast Flux Test Facility Reactor (FFTFR), Gas Cooled Fast Breeder Reactor (GCFBR). A number of papers[1,2,4-6] have been published high lighting the mechanical properties of these steels However, very few publications appeared in literature which can highlight the mechanical properties of modified 9 Cr-1 Mo steel with respect to oxidation Present work has been carried out keeping this in view.

Various mechanical properties, tensile, fatigue, creep-fatigue, stress-rupture, of modified 9 Cr-1 Mo steel (after oxidation) has been studied at temperature ranging from 25°C to 540°C

The literature survey made on these steels and related alloy steels is summarised below

1 1 Constitution of Alloy

Growing importance of ferritic steel in nuclear power generating system, an stringent composition of alloy is needed For the high temperature oxidation resistant steel, the carbon content should be kept as low as possible[11] A minimum amount of Cr, between 8 and 16%, must be present in Fe-Cr alloy to produce a scale, protective in temperature range 647-947°C[12,13]. Mo is strong carbide former, so its addition in small amount 0 5 - 1.0% (sufficient to combine with carbon) gives higher oxidation resistance, improved creep strength and tensile strength of steel[14], but higher percentage of Mo at 900°C leads increased rate of oxidation due to cracking of scale[11] Vanadium and niobium are stronger carbide former, even small amounts less than 1% can be important. They improve the high temperature mechanical properties[14]. Higher silicon content of steel shows beneficial result for oxidation at 800-900°C[11] But its higher content

also leads to high ductile to brittle transition temperature (DBTT) and low impact energy, early onset of the tertiary creep[1,14], so optimum Si content is required Therefore this led to development of modified 9 Cr-1 Mo ferritic steel.

1 2 Heat Treatment and Microstructure

Depending upon the use of the steel, three different heat treatments are in practice, full annealing for construction material, Isothermal annealing for pipes, normalizing and tempering for forgings and plates. The modified alloy is also recommended for use in normalized and tempered condition (1040°C for 1 hr, air cooled to room temperature, 760°C for 1 hr, air cooled to room temperature)[1,4-6]

Figure 1 1 shows austenitic microstructure of modified alloy (net Cr ≡ 11 35%) at about 900°C. A normalizing temperature 1040°C, a little higher than for conventional alloy steels was applied to dissolve niobium carbide and vanadium carbide, resulting into improved hardenability[5], so air cooling from 1040°C to room temperature results into martensitic structure and tempering at 760°C will result into tempered martensitic structure (ferritic) with fine carbide precipitates of $M_{23}C_6[(Cr,Fe,V)_{23}(C,N)_6]$ and MC $[Nb(C,N)]$[1,5,6].

Sikka et al.[1] reported that a decrease of 14 to 28°C in tempering temperature from 760°C substantially increased

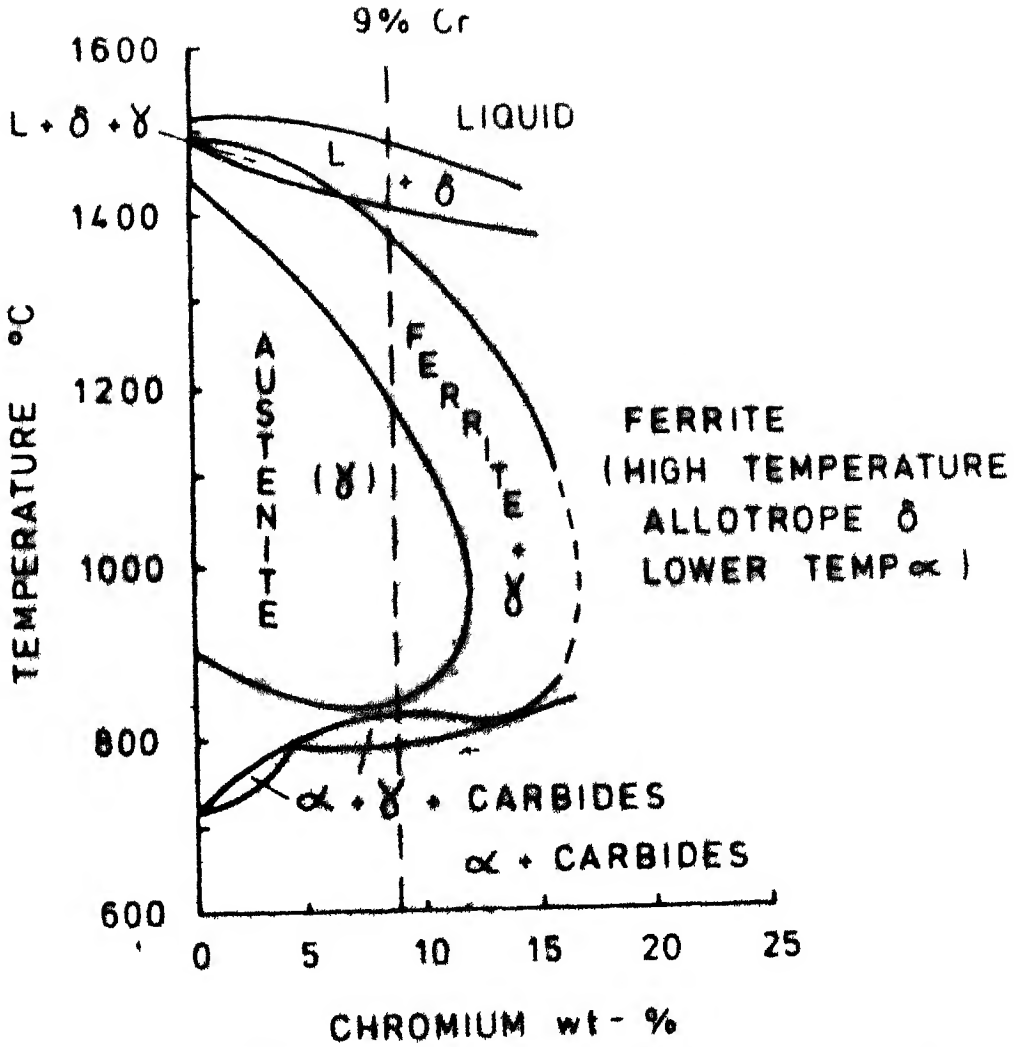

Fig 11 Schematic Pseudo-Equilibrium Phase Diagram for 0.1 C Steels (Ref 24)

yield strength and ultimate tensile strength for test temperatures through 427°C

1 3 Oxidation of Iron

Iron forms three stable oxides Wustite, FeO, Magnetite, Fe_3O_4, and hematite, Fe_2O_3 The oxide formed on iron depends upon the temperature of oxidation process The iron-oxygen equilibrium diagram is shown in Fig 1.2 FeO is a p-type conductor The defects consist of vacant cation sites and an equivalent number of electron defects, represented chemically trivalent Fe^{3+} ion Consequently high diffusion is essentially cationic via vacant cation sites. Fe_3O_4 also exists with an excess oxygen, but the excess is much smaller than wustite, and correspondingly less defect concentration[11]. Both cations and anions diffuse in Fe_3O_4. Hematite is an n-type conductor in which anions largely diffuse[15].

Above 250°C and at normal pressure of air or oxygen, the oxidation rate of iron has been reported to be parabolic[16] It is reported that upto 900°C, most of the scale consists of FeO and at this temperature, the amount of Fe_3O_4 and Fe_2O_3 starts to increase rapidly Tasche[17] has reported that below 625°C the scale is one layered and consists of essentially of Fe_3O_4 Above 625°C the oxide occurs in two layers where FeO is adjacent to metal and Fe_3O_4 composes the outer layer. The growth of oxide takes place by ionic

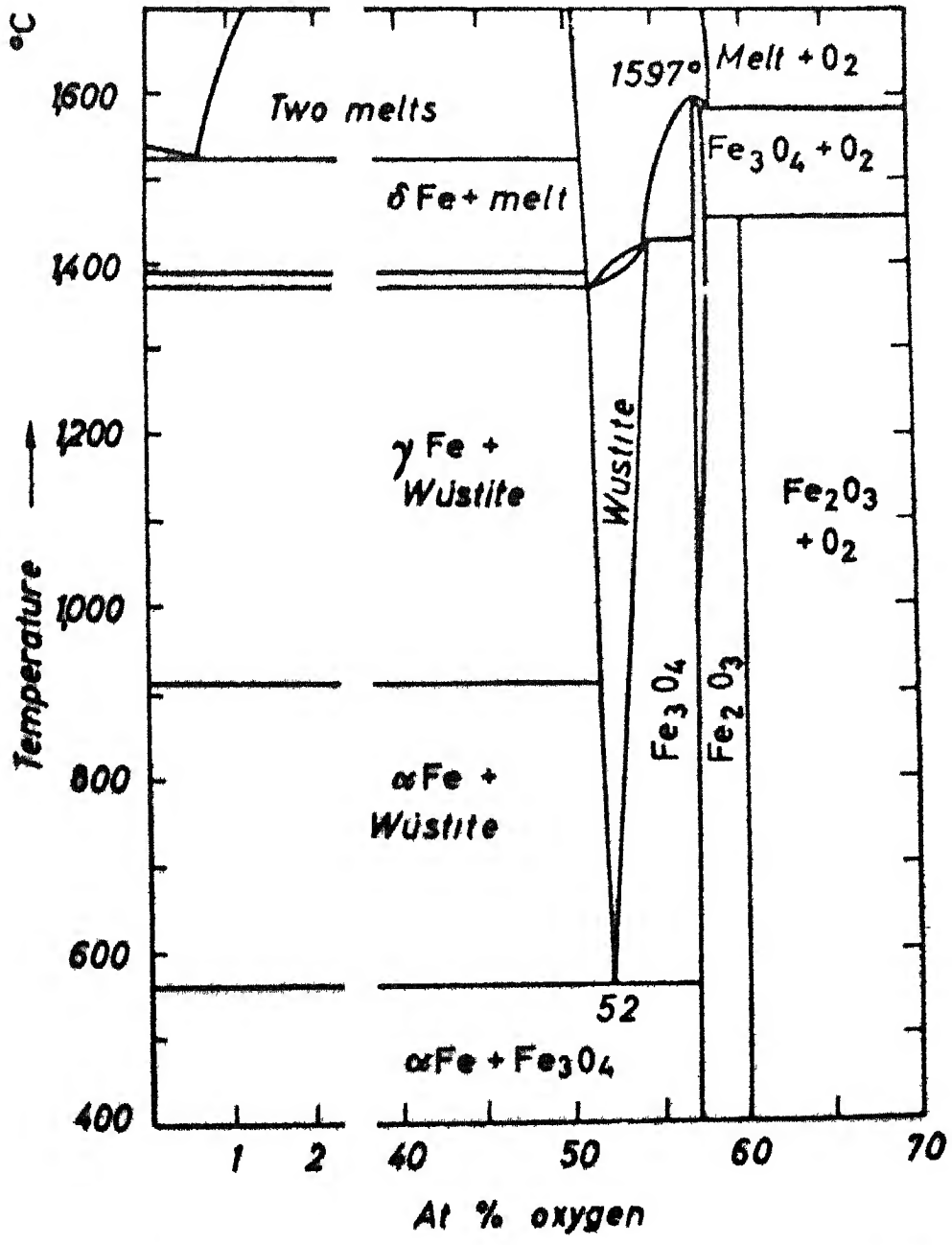

Figure 1 2 Equilibrium diagram of the iron-oxygen system (Ref 11)

diffusion and thickness of each layer in the oxide scale is determined by the ionic diffusion through that layer Simplified picture in Fig 1 3 emerges for oxidation mechanism of iron above 600°C However diffusion of oxygen in FeO and in Fe_3O_4 can not be ruled out

Effect of oxygen pressure on the oxidation of iron was studied by Caplan et al.[15] at 500°C They found that oxidation was lower at 10 torr than at 760 torr owing to greater separation between oxide and metal

It is reported that cold work iron oxidizes faster than annealed iron Since, Fe_3O_4 formed on cold work iron either has leakage paths for easy diffusion or a steep cation vacancy gradient or both[18].

1.4 Oxidation of Alloy Steel

Ferritic steel depends for their corrosion resistance on the formation of a thin protective layer oxide scale, normally consisting of either Cr_2O_3 or a spinel containing small amounts of iron, and other alloying addition[11] If this layer is disrupted by excessive oxidation or destroyed by constituents of envrionment, the oxidation resistance of that alloy is severely diminished Ferritic steels consists of chromium and molybdenum. At low Cr content of steel, both chromium rich and iron rich oxides form on the surface Some chromium will enter solution in FeO phase due to stability

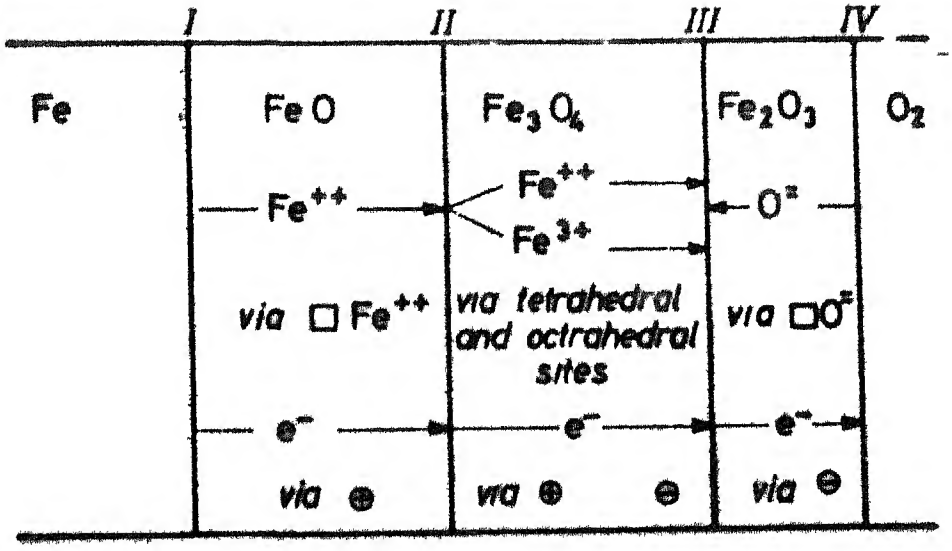

Phase boundary reactions

I $Fe + [\square\ Fe^{++} + 2\oplus]_{FeO} = zero$

II $Fe_3O_4 = [4\ FeO + \square\ Fe^{++} + 2\oplus]_{FeO}$
$[\oplus]_{FeO} + [\square\ Fe^{++} + \square\ Fe^{3+}]_{Fe_3O_4} = 2[Fe^{++}]_{FeO}$

III $12\ Fe_2O_3 = 9\ Fe_3O_4 + [\square Fe^{++} + 2\ \square\ Fe^{3+} + 8\oplus]_{Fe_3O_4}$
$2\ Fe_3O_4 = 3\ Fe_2O_3 + [\square\ O^{=} + 2\ominus]_{Fe_2O_3}$

IV $\frac{1}{2}(O_2) + [\square O^{=} + 2\ominus]_{Fe_2O_3} = zero$

Figure 13 Oxidation mechanism of iron above 600°C (Ref 11)

of spinel The solubility is limited An increase in rate constant is rarely observed On increasing Cr content, Fe^{2+} ions are progressively blocked by $FeCr_2O_4$ islands, and the FeO layer correspondingly becomes thinner relative to Fe_3O_4 layer thickness but still reaction rate is quite fast and typical of pure iron When the Cr content is increased further, a scale of mixed spinel Fe (Fe, Cr)$_2O_4$ is produced and the parabolic rate constant is lowered Iron ions are much more mobile in this oxide than Cr^{3+} ion So at longer time quite pure oxides can be found at the outer surface of the scale when the oxidation rate is controlled by diffusion of iron ions through the inner mixed spinel layer. The parabolic rate constant shows a minimum at 16-22% Cr for all temperature, 923 to 1223°K[12,13] A minimum amount of Cr (between 8 and 16%) must be present in Fe-Cr alloy to produce a scale which is protective in the temperature range 920 - 1220°K.

Small concentration of Mo, upto a few percent, some what improves the oxidation resistance of iron at 600-1000°C Vanadium does not contribute to improvement of the oxidation of steels for high temperature oxidation resistant steel The carbon content should be kept as low as possible[12]

Verma[19] reported, Cr diffusion rates in ferritic and austenitic steels indicates that Cr depletion at corroding metal surface is greater in austenitics than in ferritics. Thus, the metallic substrate of ferritics should be

more resistant to corrosion following oxide spalling than that of austenitics resulting in delayed break away kinetics The antioxidation properties of this modified 9 Cr-1 Mo steel in steam is better than 9 Cr-2 Mo, 2 25 Cr-1 Mo, steels and comparable with that of stainless steel[1,5], but due to its low Si contents, the modified alloy revealed higher weight gain in steam at 538°C than that of standard 9 Cr - 1 Mo alloy[1]

Singh et al [8] reported oxidation of this steel in air and oxygen They found that oxidation rate constant is logarithmic from 550 to 750°C, linear or paralinear from 750 to 850°C and parabolic at 950°C

1 5 Mechanical Properties of Modified 9 Cr-1 Mo steel

Sikka et.al.[1,2,4] carried out extensive investigation at the mechanical properties of modified 9 Cr-1 Mo ferritic steel.

1 5.1 Tensile Properties

In terms of yield and ultimate tensile strengths, the modified 9 Cr- 1 Mo steel is better than standard 9 Cr-1 Mo, 2 25 Cr-1 Mo, 304 stainless steel upto 650-700°C[4,5,12]. As far as allowable stress is concerned, Fig 1.4 depicts superiority of modified 9 Cr-1 Mo over other steels Flow

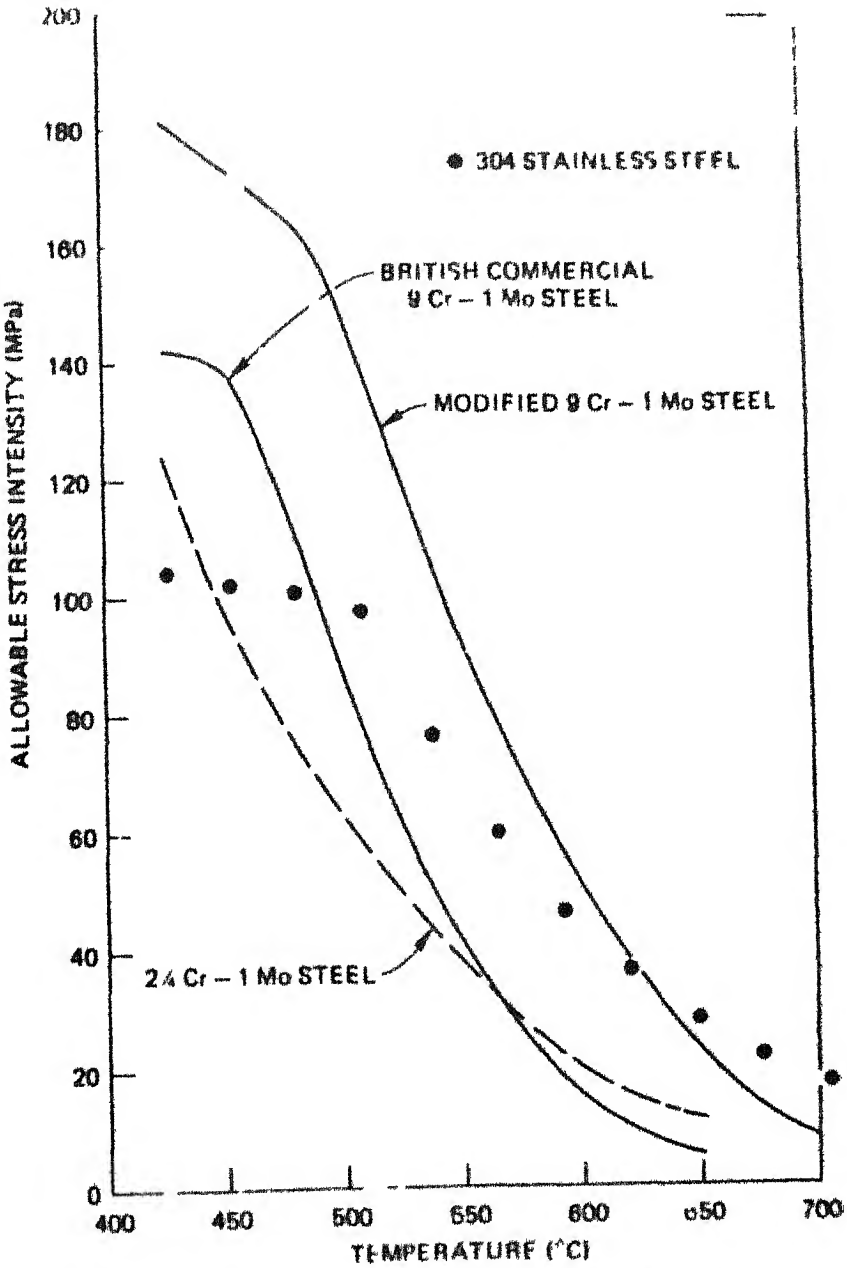

Fig 1.4 Variation of Estimated Allowable Stress Intensity with Temperature for Several Materials

(Fig 1.4)

properties are very much dependent on temperature, strength decreases and ductility increases as the temperature of test is increased[20,21,22]

From the various tensile data for the modified 9 Cr-1 Mo steel, Brooker et al [4] worked out the mathematical models to fit with yield strength and ultimate tensile strength

$$\log \sigma_u = C_h^u = 1\ 010\times10^{-3}T + 4\ 152\times10^{-6}T^2 - 5\ 644\times10^{-9}T^3$$

and

$$\log \sigma_y = C_h^y - 1\ 508\times10^{-3}T + 6.15\times10^{-6}T^2 - 7.481\times10^{-9}T^3$$

where σ_u is ultimate tensile strength (MPa), σ_y is 0.2% off set yield strength (MPa), and T is temperature (°C) (All logarithms are base 10) The term C_h^u and C_h^y are lot constants, which reflect lot to lot variability in UTS and yield strength, respectively.

1 5.2 Hardness

Tempering temperature affects largely the hardness of modified 9 Cr-1 Mo steel[1] The as-hardened hardness of modified 9Cr-1Mo is higher than that of standard 9Cr-1Mo and lower than that of 12 Cr- 1 Mo (HT9) The higher hardness of modified 9Cr-1Mo than standard 9Cr-1Mo is probably due to its finer grainsize The higher hardness of HT9 than

standard and modified 9Cr-1Mo steel is due to low carbon content in later The peak hardness of this steel is observed at 510°C The peak temperature and hardness for modified 9Cr-1Mo steel are higher than those of standard 9Cr-1Mo steel The peak hardness of 12Cr-1Mo is higher than that of modified 9Cr-1Mo and peak temperature is nearly same.

The tempered hardness at 760°C of modified 9Cr-1Mo is about the same as observed from standard 9Cr-1Mo steel The tempered hardness of 12Cr-1Mo is higher than those of both standard and modified 9Cr-1Mo steel This is expected from the amount of carbides present in HT9 as compared with 9Cr-1Mo steels.

1 5 3 Fatigue and Creep-Fatigue

Sikka et al [1] study revealed that modified alloy has about the same fatigue strength as type 316 stainless steel in the range of 525 to 593°C. The alloy also has superior fatigue life beyond 10^4 cycles to 2 25 Cr-1Mo, standard 9Cr-1Mo and type 304 stainless steel. Jones[6] carried out the study about the microstructural changes of this steel during cycling Very little microstructural evolution occurs in 1000 hr at 538°C without cycling while extensive changes occur with cycling The synergism between temperature and mechanical cycling accelerates the

development of equiaxed subgrains with low dislocation density and much coarsened MC and $M_{23}C_6$ carbides. This evolution in substructure changes the dominant strengthening mechanism from dislocation substructure and precipitation hardening to interaction solid solution strengthening from Mo and V An increase in amount of Mo in $M_{23}C_6$ carbides indicates that longer duration creep-fatigue tests would yield even more softening.

1.5.4 Creep Strength

Creep-rupture properties of ferritic steels have been studied extensively by several workers[1,5,23] Sanderson[24] carried out stress rupture tests for 9Cr-2Mo, variants steels, at 550°C both of them exhibited a superior rupture strength to 9Cr-1Mo steel, their increased alloy content-allowing elevated temperature strengthening by solid solution and dispersion hardening mechanism

In 9Cr-1Mo steel creep process takes place by matrix deformation leading to localized areas of a highly recovered dislocation mesh. Within these locally recovered regions, secondary precipitation of an M_2 X dispersion takes place No evidence of grain boundary sliding or cavitation in temperature range 475-550°C had been found[23,24]

Sikka et al.[1,4] reported that modified 9Cr-1Mo steel has creep strength that exceeds that of standard and modified

steels in the range 2 2 to 12% Cr-Mo for the entire temperature range (427-704°C) The modified 9Cr-1Mo steel shows creep-rupture strength comparable to that of type 304 stainless steel upto about 625°C The modified alloy also possesses superiority over other ferritic steels in regard to ductily to creep rupture

Booker et.al.[4] worked out an mathematical model for creep-rupture data for modified 9Cr-1Mo steel as

$$\log t_r = C_h + a_1\sigma + a_2 \log\sigma + a_3/T$$

where,

t_r = rupture life (h),

σ = stress (MPa),

T = temperature (K),

a_1-a_3 = regression constants

C_h = lot constant

1.6 Impact Properties

Impact properties of modified 9Cr-1Mo steels has been compared with that of standard 9Cr-1Mo steels Sikka et al [1] carried out the impact test for modified 9Cr-1Mo and standard 9Cr-1Mo steels DBTT of modified 9Cr-1Mo is lower than that of standard 9Cr-1Mo steel Impact energy for modified alloy is better than the standard alloy. Si content affected the charpy properties.

The lower Si produces lower transition temperature and higher impact energy Higher impact strength of modified 9Cr-1Mo steel is attributed to low Si content and finer grainsize

It is evident from literature review that no study of the effect of structure on mechanical properties of this steel has been done under the oxidized condition Hence, it was thought desirable to investigate the effect of structure of the steel, on the mechanical properties under oxidized condition

CHAPTER 2

EXPERIMENTAL

2 1 Material

Modified 9Cr-1Mo steel was obtained from Oak Ridge National Laboratory, Tennessese, U S A through kind courtesy of Mr Ashok K.Khare, Chief Metallurgist National forge Company Pennsylvania, U S A in the form of 1 cm thick plate The chemical composition of alloy is given below

Element	C	Mn	Si	S	P	Cr	Mo	V	Nb	N	Ni	Fe
wt pct.	083	.46	.41	.004	010	8 46	1 02	198	.072	051	.09	Balance

2 2 Processing of the Material

The received alloy was annealed (850°C for 1h and furnace cooled to room temperature) in vacuum (10^{-3} mm of Hg) and then cold rolled to approximately 1 mm thickness without any intermediate annealing

2 3 Specimen Preparation

Rectangular strips with the longitudinal axis parallel to the rolling direction were cut from the cold rolled sheet followed by degreasing and annealing in vacuum (10^{-3} mm of Hg) (850°C for 1h and furnace cooled to room temperature) The specimens as shown in Fig 2 1 were made for mechanical testing.

Two different treatments were given to specimens. Specimens were normalized and tempered in vacuum of 10^{-3} mm of Hg (1040°C for 1 h, air cooled to room temperature, 760°C for 1h, air cooled to room temperature). Few specimens were annealed and normalized (850°C for 1 hr, furnace cooled to room temperature, 760°C for 1h, air cooled to room temperature) Finally the specimens were polished from both the sides upto 4/0 energy paper and washed with distilled water and acetone before using in experiment. After this specimens were weighed using microbalance having readability of 0.05 mg.

2.4 Oxidation in Oxygen

Figure 2 3 shows the view of system used for oxidation and heat treatment. Three samples were oxidized simultaneously. The free suspension of each sample, was achieved by hanging them from the hookes attached with platinum ring which in turn was suspended from the top of the

quartz reaction chamber by another platinum wire The furnace used had kanthal wire winding with uniform temperature zone controlled within $\pm$ 4°C A screw jack was used to move the furnace up and down The whole system was evacuated using mechanical pump to a vacuum better than 10^{-3} mm of Hg and then flushed three times with commercial oxygen obtained from Indian Oxygen Limited, in order to remove the air impurities and then filled with oxygen at pressure slightly less than 1 atm. When required temperature, 650°C is reached in the uniform temperature zone of furnace The quartz reaction chamber is brought in the uniform temperature zone of furnace with the help of screw jack At this temperature oxygen pressure inside the system rose slightly above the 1 atm (1 atm + 3-5 mm of Hg) which avoids even minor leakage of air into system The samples were oxidized for varying times 30, 60, 90 minutes, in order to get required oxygen in sample, as the oxidation for 3 hrs at 650°C resulted into surface buckling

At the end of each run the furnace was lowered and the samples were allowed to cool in the same reaction chamber. Finally, the samples were removed from the system and the weight increase of the individual sample and the physical appearance was noted.

2 5 Mecnanical Testing

2,5 1© Tensile Testing

All tensile testings upto 540°C were carried out with Instron 1195 model A cylindrical furnace with kanthal wire winding was used to get the desired temperature Required temperature profiles were obtained by varying voltage and current settings Fig 2 2 shows the temperature profiles of the successful runs Tensile tests were carried at four temperatures, 25°C, 203°C, 425°C, 540°C Samples of four different oxygen concentration (in the range of 0 to 0 05% oxygen) tested at each temperature in the air For high temperature test, bead of chromel-alumel thermo-couple was tied at gauge region inorder to get spot recording of temperature and sample was mounted in the train assembly with the help of hot die steel grip The temperature variation during test at the gauge region was $\pm$4°C. The strain rate and the chart speed were constant throughout the tensile testing and they were 1.66×10^{-3}/sec and 20mm/min After sample failure, it was removed from Instron machine and cross-section at fracture was measured with the help of travelling microscope.

2,5 2 Fatigue and Creep-fatigue Testing

Low cycle fatigue tests for four different oxygen content carried out with 810 Material Testing System. The samples were repeatedly cycled with minimum and maximum load

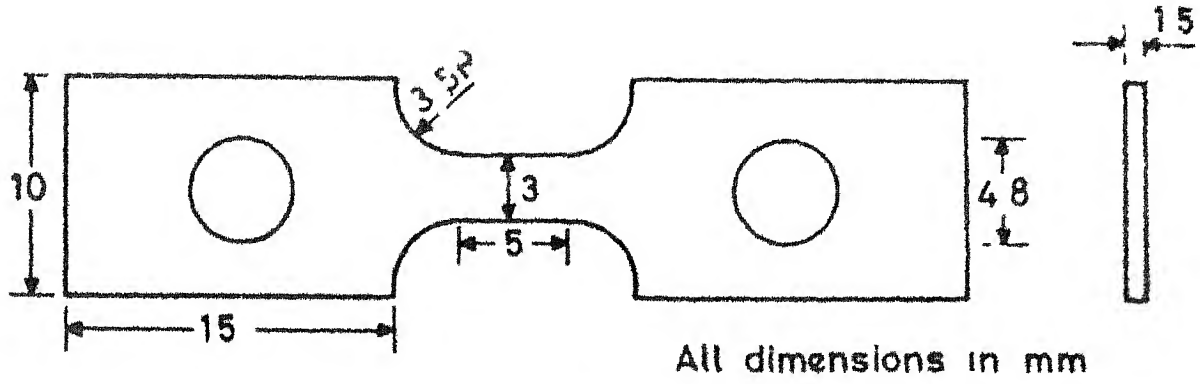

Fig 2 1 Sample design

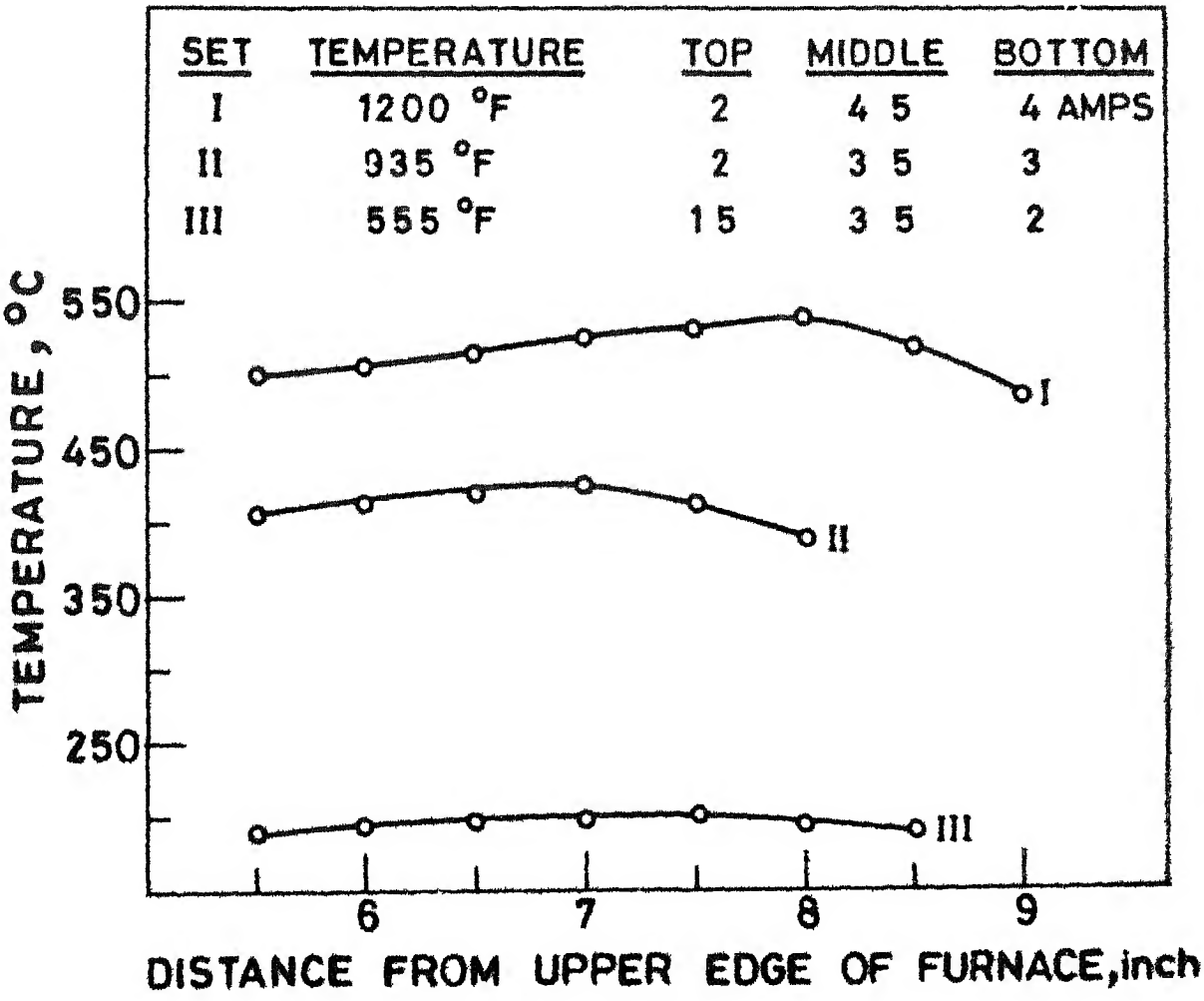

Fig 2 2 Temperature profiles of furnace at various settings of variacs

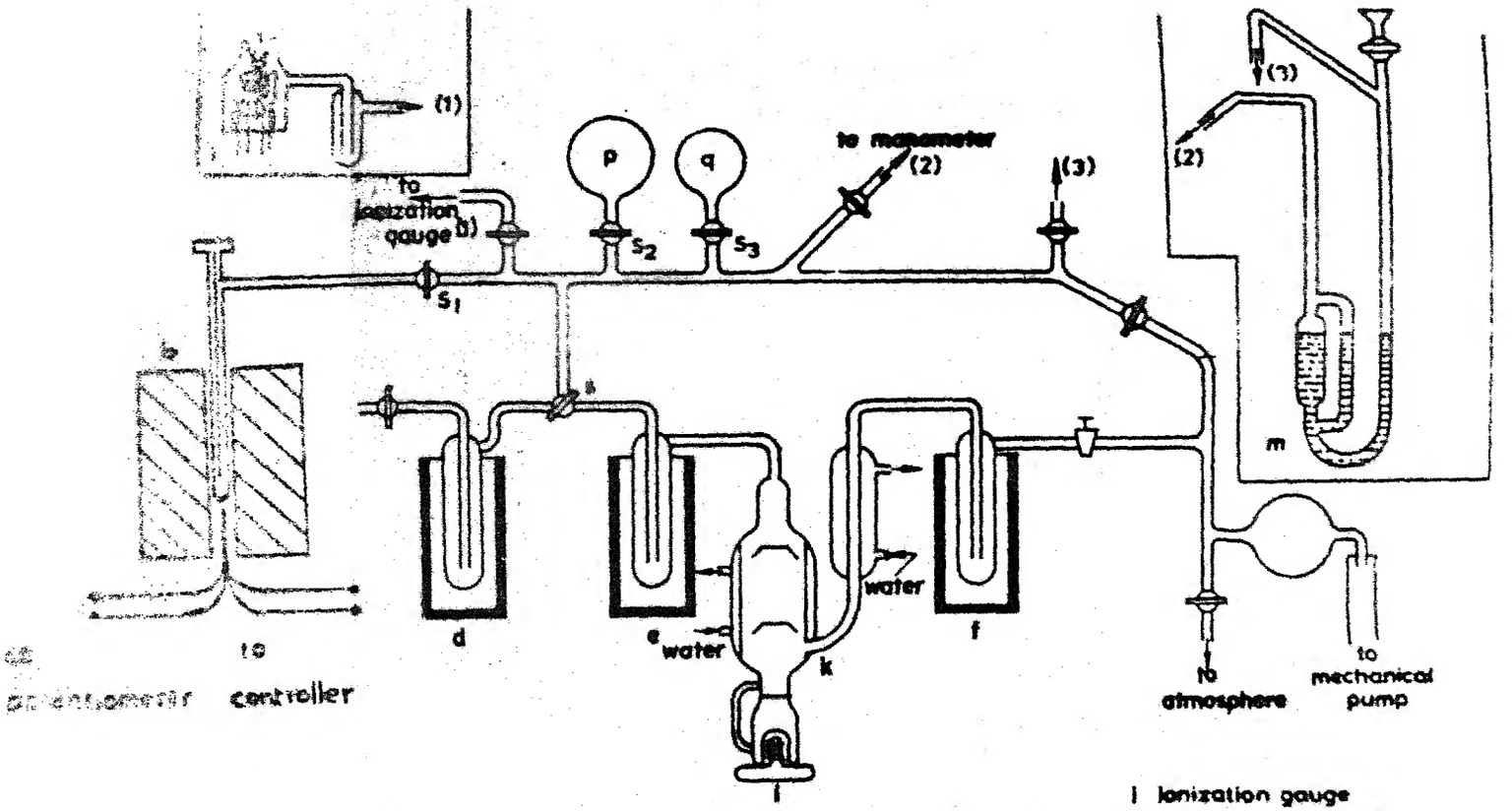

l ionization gauge
m mercury manometer
,b,c resistance furnaces
d ,e,f liquid nitrogen cold traps
g ground glass joint with water cooling arrangement
h specimen tube
j heater
k two stage mercury diffusion pump
s three-way stop cock
p,q calibrated h tbs

Fig. 2.3 Setup for oxidation and heat treatment.

(saw tooth type loading) in tensile region. The maximum stress was selected from tensile test results (46 Kg/mm^2 for annealed and normalized, 72 Kg/mm^2 for normalized and tempered) The ratio of maximum stress to minimum stress and frequency of cycling were kept constant throughout the testing as 10 and 30 cycle/sec respectively Tests were carried out till the failure of samples and correspondingly number of cycles to failure were recorded

Creep-fatigue test was carried out at 540°C with same Instron machine Mounting and testing of sample were done in the similar way as that in tensile testing Ratio of minimum stress to maximum stress and cross-head speed were kept constant throughout the testing, 0 1 and 10 mm/min. respectively in this case also The frequency of cycling was calculated which varied from sample to sample due to variation in cross-section area of gauge region Total number of cycle and time to failure for each sample were recorded

2 5 3 Stress-rupture Testing

Stress-rupture tests at 540°C for four different oxygen concentration, were carried out with SATEC System Various trail settings for voltage and current were done for three zones of furnace (Kanthal wiring) in order to get 540°C at the sample gauge region. Thermocouple bead was

tied to gauge region of sample so that spot temperature could be recorded The temperature variation during test was ± 3°C Three trail runs were made at various stress and then initial applied stress 28 Kg/mm^2 was selected based on trials Sample was mounted in assembly, and furnace was put on As soon as required temperature of 540°C is reached, the stress is applied carefully, and timer is put on Instant elongation is noted using Cathedometer (readability 0.01 mm) which was preset on the specific mark on the assembly Intermittent elongation was recorded till the rupture takes place At the instant of rupture, machine stops automatically and gives the time to rupture (creep is occurring continuously, instant the load is applied but increase in strain is not measurable unless certain increment in strain (not known) at which motor runs to make assembly vertical).

2 6 Optical Microscopy (Metallography)

Mechanical tested samples were mounted on perspex slabs using adhesive tapes They were polished up 4/0 emery paper to remove the oxide from surface and the polished on wheel, using 1 µm alumina suspension The polished surface of sample was the etched with picrol (1%) for 20-40 seconds and examined under the optical microscope and the microstructures were photographed.

2 7 Fractography (S.E M.)

The fracture surfaces of mechanical tested samples were examined in the scanning electron microscope An aluminium sample holder with a slit to accomodate the sample and a secrew to hold intact was made The whole fracture surface was scanned and the notable features were photographed

2 8 X-ray Diffraction

X-ray diffraction runs were taken by diffractometer for two samples, unoxidized sample, tested at room temperature, oxidized and stress-ruptured (540°C) sample Copper with filter, was used as target material Continuous recording of 2θ vs Intensity was made by diffractometer

2 7 Fractography (S.E M)

The fracture surfaces of mechanical tested samples were examined in the scanning electron microscope An aluminium sample holder with a slit to accomodate the sample and a secrew to hold intact was made The whole fracture surface was scanned and the notable features were photographed.

2 8 X-ray Diffraction

X-ray diffraction runs were taken by diffractometer for two samples, unoxidized sample, tested at room temperature, oxidized and stress-ruptured (540°C) sample. Copper with filter, was used as target material Continuous recording of 2θ vs Intensity was made by diffractometer.

CHAPTER 3

RESULTS AND DISCUSSION

Various terms and mathematical formulae used in this work are defined briefly as follows

The maximum load which the specimen can with stand without failure is called the load at ultimate tensite strength and corresponding stress

$\sigma_u = \frac{P_{max}}{A_o}$ is called ultimate tensile strength or tensile strength The yield strength is the minimum stress at which specimen is deformed (yield) without a noticeable increase in load The offset yield strength is determined by the stress correspondingly required for getting 0.2 percent off-set strain.

$$\sigma_o = \frac{P_{(\text{strain off-set} = 0.002)}}{A_o}$$

Ductility is the measurement of the ability of the metal to flow before fracture. The conventional measures of ductility that are obtained from the tension test are the engineering strain at fracture e_f (usually called the elongation) and the reduction of area at fracture q

$$e_f = \frac{L_f - L_o}{L_o}$$

$$q = \frac{A_o - A_f}{A_o}$$

where L_f, L_o are fractured and original length and A_f, A_o are fractured and original cross-sectional area respectively

Uniform strain is based on the strain upto maximum load It represents the elongation just before start to necking Fracture strength, is the load corresponding to fracture point divided by original cross sectional area

$$\sigma_f = P_f/A_o$$

Actually metal continues to strain harden all the way upto fracture, so that the stress required to produce further deformation should also increase So true fracture stress is the load at fracture divided by the cross-sectional area at fracture

$$S_f = \frac{P_f}{A_f} = \frac{P_f}{A_o} \times \frac{A_o}{A_f} = \sigma_f \times \frac{1}{1-q}$$

The true fracture strain E_f is the true strain based on original area A_o and area after fracture A_f

$$E_f = \ln \frac{A_o}{A_f} = \ln \frac{1}{1-q}$$

Stress applied for fatigue test is represented by

stress ratio R

$$R = \frac{\sigma_{min}}{\sigma_{max}}$$

where σ_{max} is maximum stress and σ_{min} is minimum stress in the repeated stress cycle

In the coaxing, specimen is tested for large number of cycles below fatigue limit and the stress is increased in small increments after allowing a large number of cycles to occur at each stress level

The results of various mechanical tests of modified 9Cr-1Mo steel are summarized and discussed here

3 1 Results

3 1 1 Tensile Test

The data obtained from the load vs elongation plot of INSTRON at various temperature, oxygen concentration are shown in Appendix-A (Table 1-8) Variation in ultimate tensile strength, for both normalized and tempered, annealed and normalized condition, with oxygen concentration at various temperature are shown in Figures 3 1 and 3 9 respectively A general features observed are that the tensile strength decreases with temperature This is in agreement with the results obtained by Sikka et al [1]

When the temperature is raised 540°C from 425°C, the tensile strength drops considerably. The tensile strength decreased slightly with increase in the oxygen concentration at the test temperature. Normalized and tempered steel has shown higher strength than that of annealed and normalized steel

The variation of yield strength with oxygen concentration, at various temperatures are given in Figures 3 2 and 3 10 for normalized and tempered, annealed and normalized samples Similarly, Figures 3.3 and 3 11 depict the variation of engineering fracture strength with oxygen concentration at various temperature for normalized and tempered, annealed and normalized samples The plots for yield strength, fracture strength show similar features as that of ultimate tensile strength plots.

The plots for change in true fracture strength with oxygen content at various temperature, for normalized and tempered, annealed and normalized samples are shown in Figures 3 4 and 3.12. They depict large scattering in the strength so it is not possible to draw any inference

The figures3 5 and 3 13 indicate the variation of total elongation with oxygen concentration at various temperature, for normalized and tempered, annealed and normalized samples They show slight increase in elongation with increase in oxygen content at the temperature. In

normalized and tempered samples, total elongation increases with increase of temperature except a drop at 203°C, this is in agreement with the results of various workers[1,5], but in annealed and normalized samples, total elongation increases with increase of temperature Similar kind of features are observed with reduction of areas vs oxygen plots in Figures3 6 and 3 14, for similarly treated samples

The variation in uniform elongation with oxygen content is shown in Fig 3 7 for normalized and tempered, and Fig.3 15 for annealed and normalized samples The general feature observed is that with increase of oxygen content at the temperature, the uniform elongation increases slightly. In the normalized and tempered samples,plot for 203°C lies below 25°C, 540°C above the 25°C but below 425°C In the annealed and normalized samples, plot for 25°C lies below 425°C but above the 203°C and 540°C and plot for 203°C lies above that of 540°C

Plots for true fracture strain vs oxygen concentration at various temperature for normalized and tempered samples (Fig 3 8), annealed and normalized samples (Fig 3 16) show similar nature as their corresponding plots for total elongation variation with concentration

3.1 2 Fatigue and Creep-Fatigue Test

The results of low cycle fatigue test at 25°C for both the normalized,tempered,and annealed and normalized

samples are summarized in Table 3 1 Both type of samples show that number of cycle to failure decreases with increased oxidation

The results of creep-fatigue test at 540°C performed on the normalized and tempered samples are given in Table 3.2. It reveals that increase of oxygen concentration results in the increase of number of cycle to failure.

Table 9 (Appendix-A) shows results of tensile test at 540°C, carried out after creep-fatigue cycling at 540°C for the annealed and normalized samples With increase of maximum stress of cycling, ultimate tensile strength increases while ductility (total elongation) decreases.

3 1 3 Stress-rupture Test

The results of the stress-rupture test, at 540°C, performed on the normalized and tempered samples are given in Table 10 (Appendix-A) and creep curves for different oxygen concentration are plotted in Fig 3 17 Increase in oxygen concentration results in the increase of rupture time, increase of instantaneous strain on loading, decrease in rupture strain and secondary creep rate.

Table 3.1 Fatigue Test Results

Oxygen content wt%	Description of treatment	Frequency cycles/sec	σ_{max} stress Kg/mm^2	$R = \frac{\sigma_{min}}{\sigma_{max}}$	Cycle to failure
0	Annealed & Normalized	30	46 2	0 1	30410
0 01	Annealed & Normalized	30	46 0	0 1	21120
0 02	Annealed & Normalized	30	46 8	0 1	16300
0 03	Annealed & Normalized	30	46 0	0.1	10860
0	Normalized & Tempered	30	72.1	0 1	14100
0.01	Normalized & Tempered	30	72 0	0.1	13300
0 02	Normalized & Tempered	30	72 0	0 1	10500
0 03	Normalized & Tempered	30	72.4	0 1	6000

TABLE 3 2 The Results of Creep-fatigue at 540°C for Normalized and Tempered Samples

Oxygen content wt.%	Maximum stress σ_{max} (Kg./mm^2)	$R=\sigma_{max}/\sigma_{min}$	X-head speed (mm/mm)	Cycle rate (cycle/min)	Cycle to failure	Time to failure (min)
0 0	37 0	0 1	10	24	5013	224
	37 0	0 1	10	24	3225	149
0.01	37 5	0 1	10	23	4320	203
	37 0	0 1	10	24	7677	335
0 02	37 6	0 1	10	22	4113	202
	37 2	0.1	10	25	7916	332
0 03	37.0	0 1	10	24	Not failed upto 10^4	432*
	36 6	0 1	10	24	8352	363

* Time of cycling.

TABLE 3 3 X-ray analysis results of modified 9Cr-1Mo steel under normalized and tempered conditions

$\lambda Cu = 1\ 54A^{o}$ $\lambda = 2d \sin\theta$

Specification of specimen	2θ	$d_{A^{o}}$	Intensity	I with respect to I_{max} (100)
Unoxidized and tensile tested at 25°C	29 5	3 024	60	75
	30 2	2 956	30	37 5
	36 3	2 472	17	21 25
	39 6	2 273	16	20
	43 5	2 078	17	21 25
	44 8	2 021	80	100
	48 7	1 867	14	17 5
	65	1 433	26	32 5
Oxidized for 1 hr, stress-ruptured at 540°C	23 4	3 797	21	14
	26 9	3 310	23	15 33
	29 6	3 014	150	100
	31 3	2 854	17	11 33
	36.3	2 472	40	26 66
	39 6	2 273	52	34.66
	43 6	2 073	50	33 33
	45	2 012	48	32
	47 8	1 901	18	12
	48 8	1 864	33	22
	57 7	1 596	21	14
	65 2	1 429	30	20

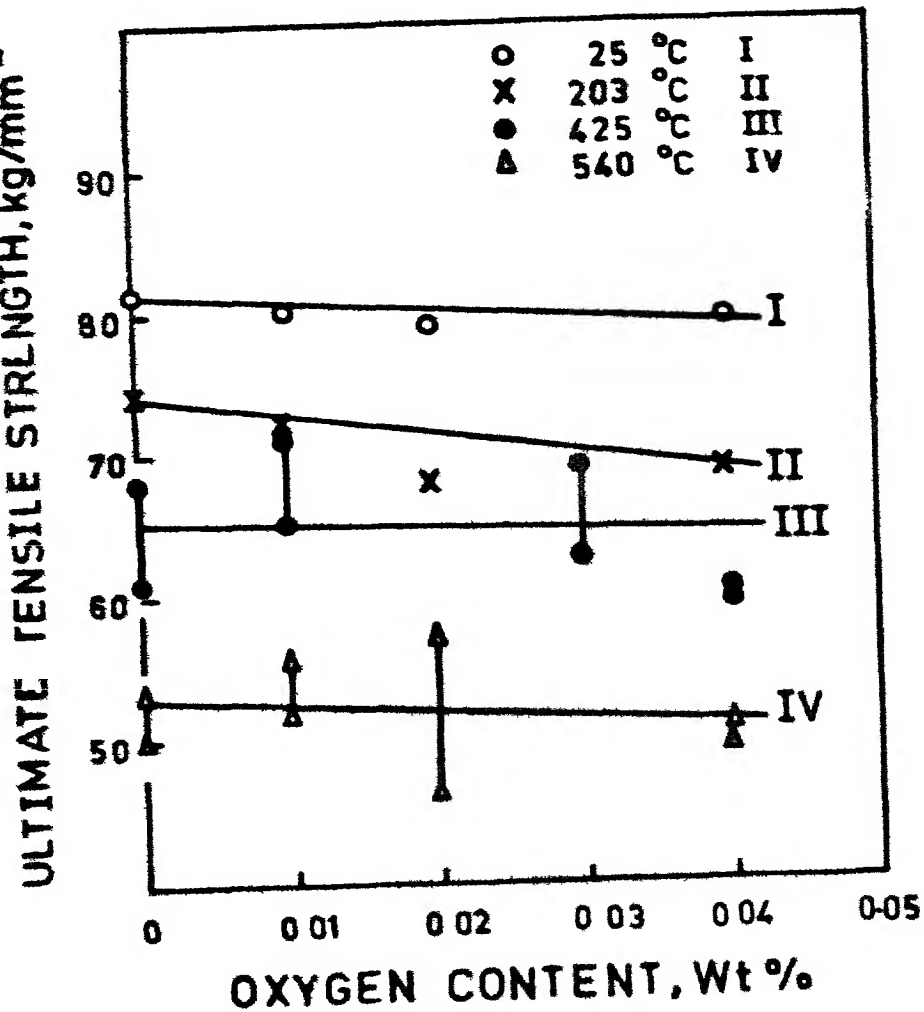

Fig 3 1 Ultimate tensile strength vs oxygen content for modified 9 Cr-1 Mo steel (normalized and tempered) at various temperatures

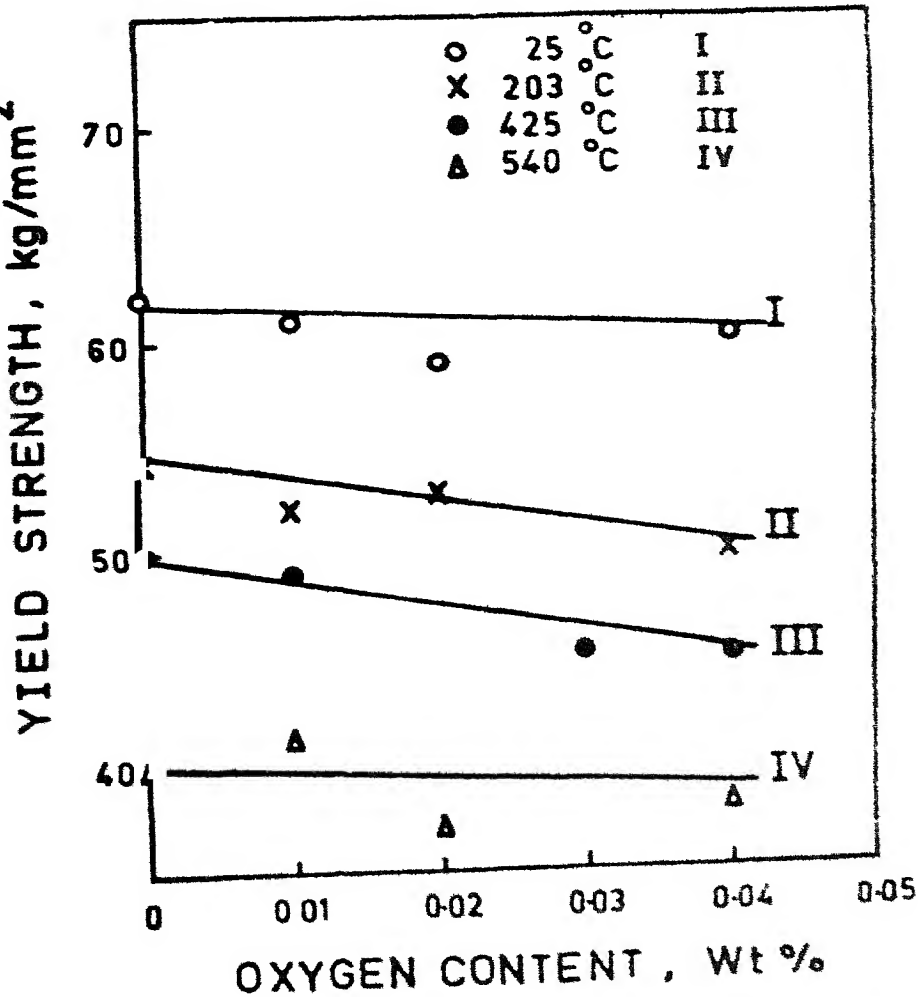

Fig 3 2 0 2% offset yield strength vs oxygen content for 9 Cr-1 Mo steel (normalized and tempered) at various temperatures (modified)

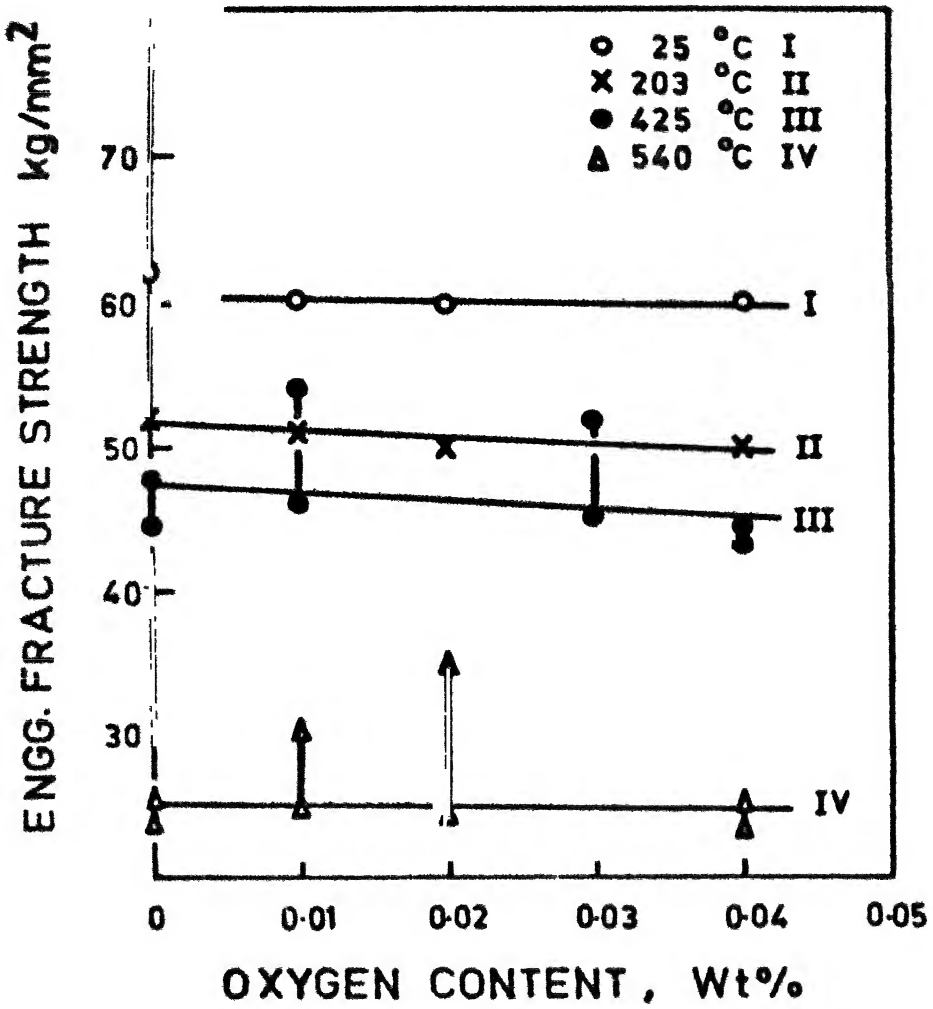

Fig·3·3 Engineering fracture strength vs oxygen content for modified 9Cr-1Mo steel (normalized and tempered) at various temperatures.

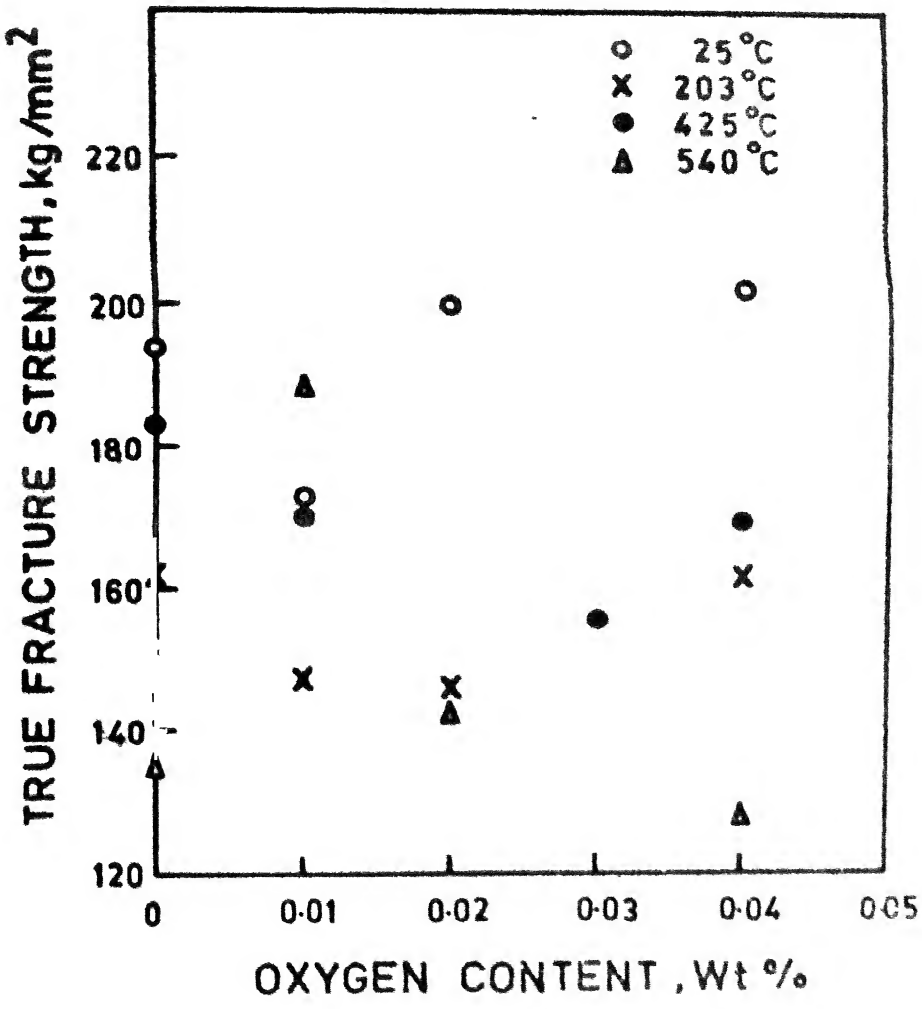

Fig·3·4 True fracture strength vs oxygen content for modified 9 Cr-1 Mo steel (normalized and tempered) at various temperatures.

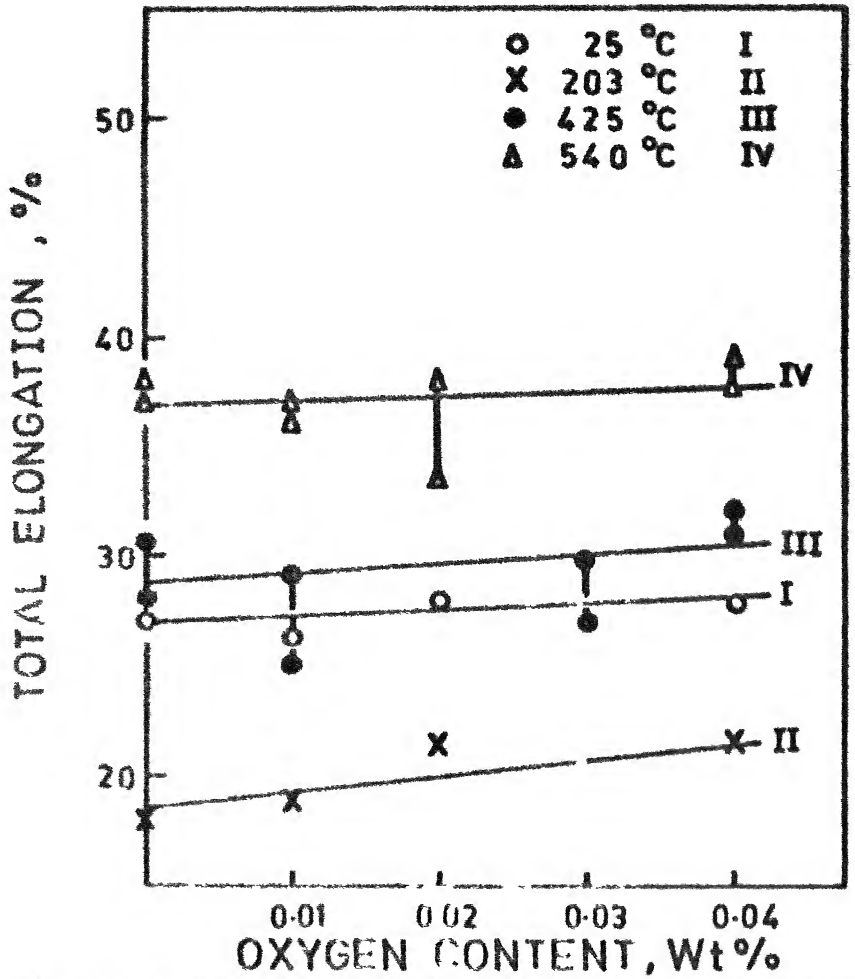

Fig·3·5 TOTAL ELONGATION VS OXYGEN CONTENT FOR MODIFIED 9Cr-1Mo STEEL (NORMALIZED AND TEMPERED) AT VARIOUS TEMPERATURES.

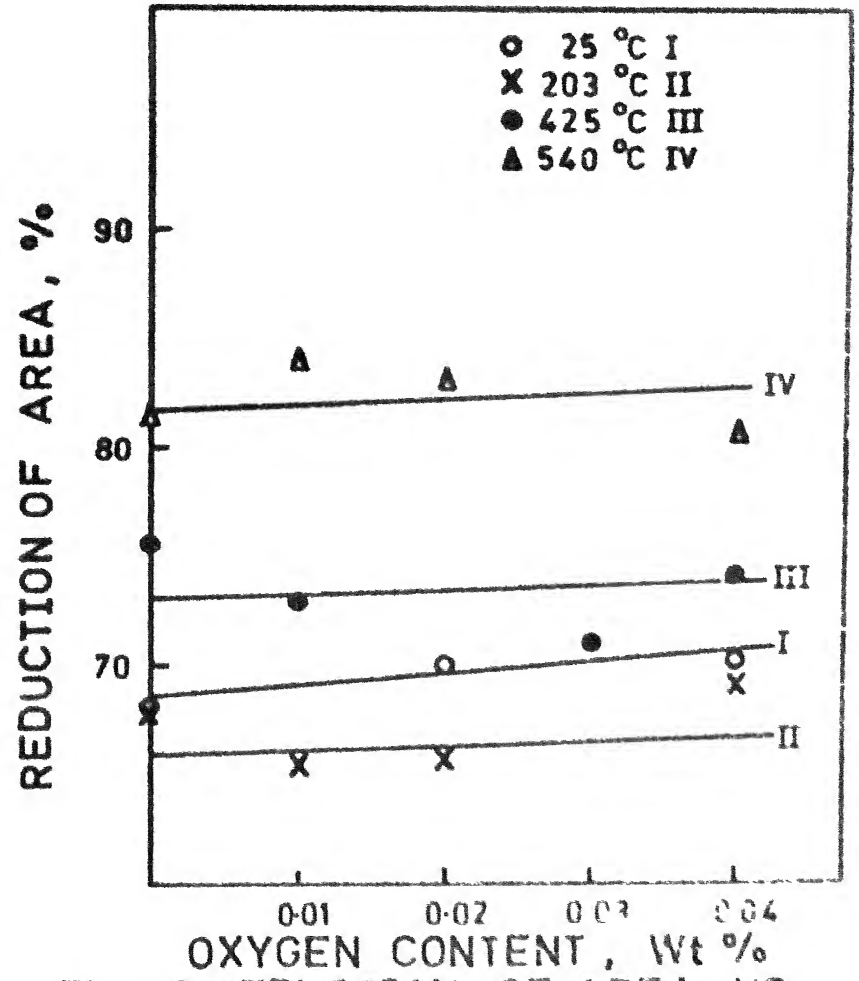

Fig·3·6 REDUCTION OF AREA VS OXYGEN CONTENT FOR MODIFIED 9Cr-1Mo STEEL (NORMLIZED AND TEMPERED) AT VARIOUS TEMPERATURES.

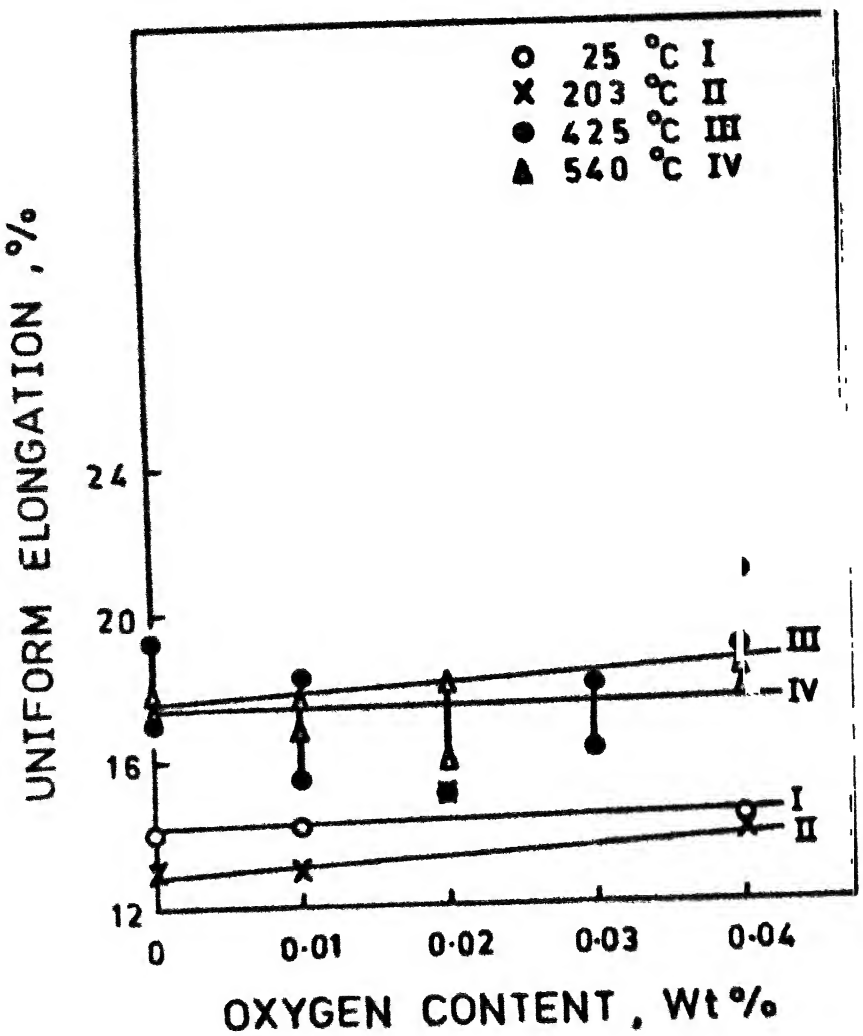

Fig·3·7 Uniform elongation vs oxygen content for modified 9Cr-1Mo steel (normalized and tempered) at various temperatures.

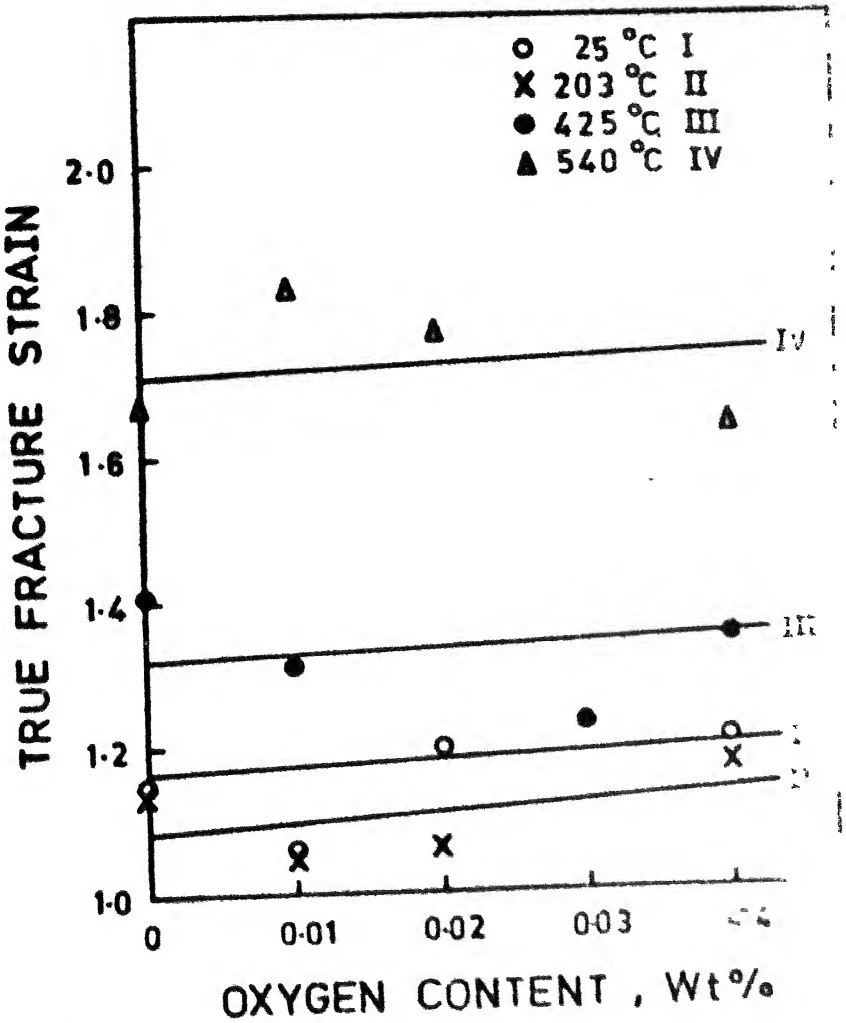

Fig·3·8 True fracture strain vs oxygen content for modified 9Cr-1Mo steel (normalized and tempered) at various temperatures.

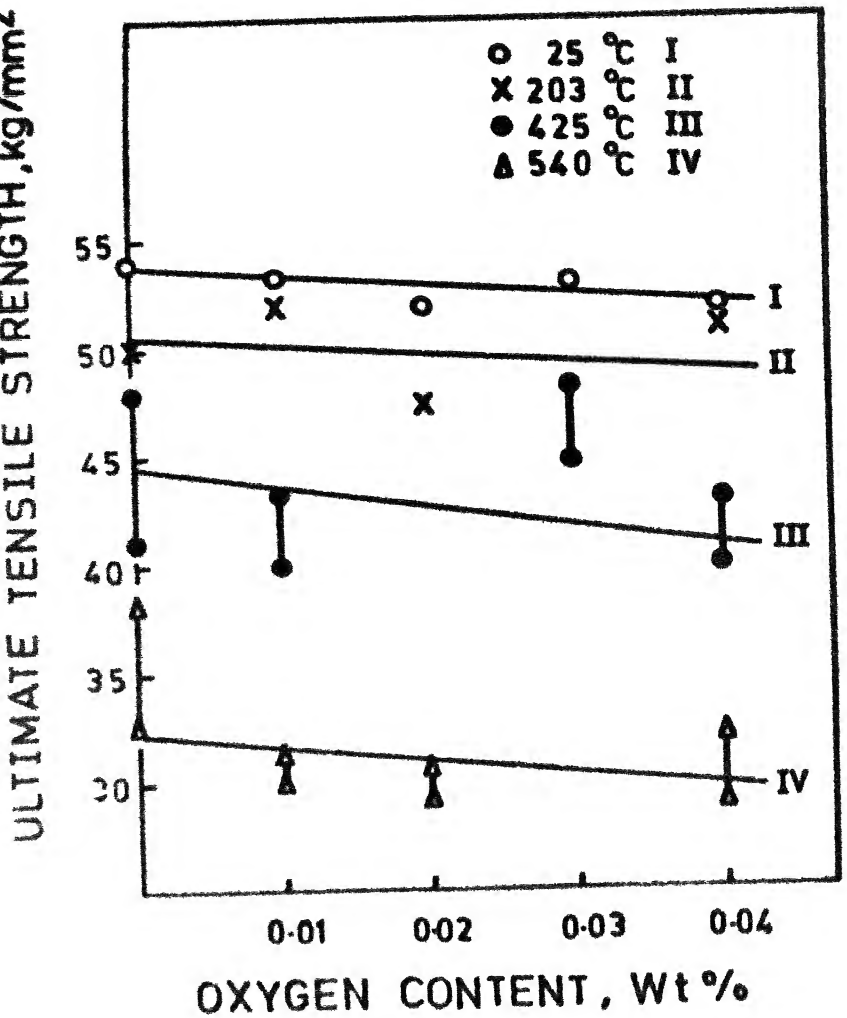

Fig·3·9 Ultimate tensile strength vs oxygen content for modified 9Cr-1Mo steel(annealed and normalized) at various temperatures.

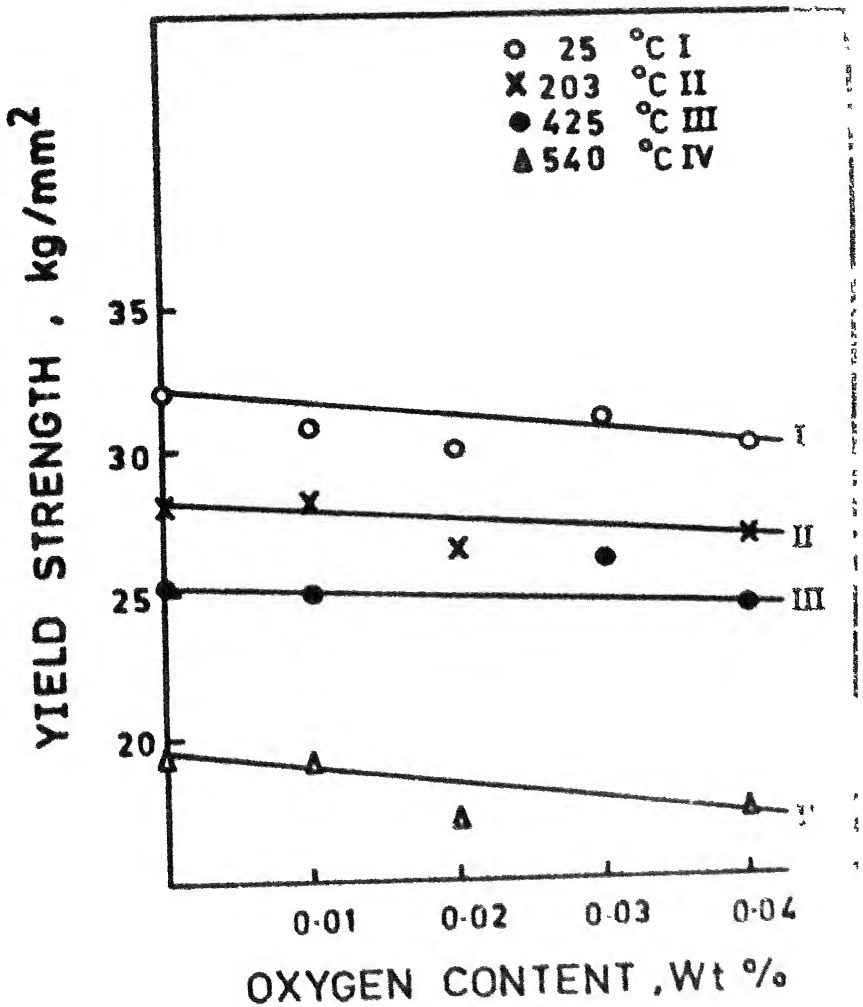

Fig·3·10 0·2% offset yield strength vs oxygen content for modified 9Cr-1Mo steel(annealed and normalized) at various temperatures.

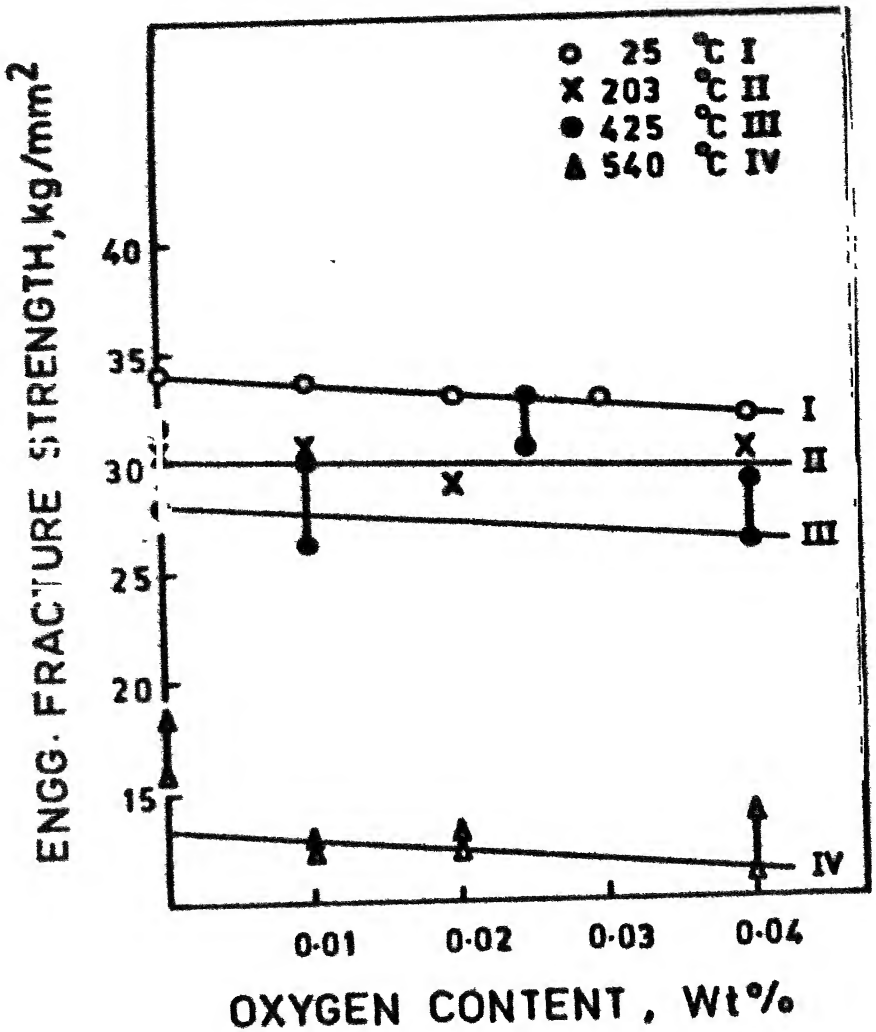

Fig·3·11 Engineering fracture strength vs oxygen content for modified 9Cr-1Mo steel(annealed and normalized) at various temperatures.

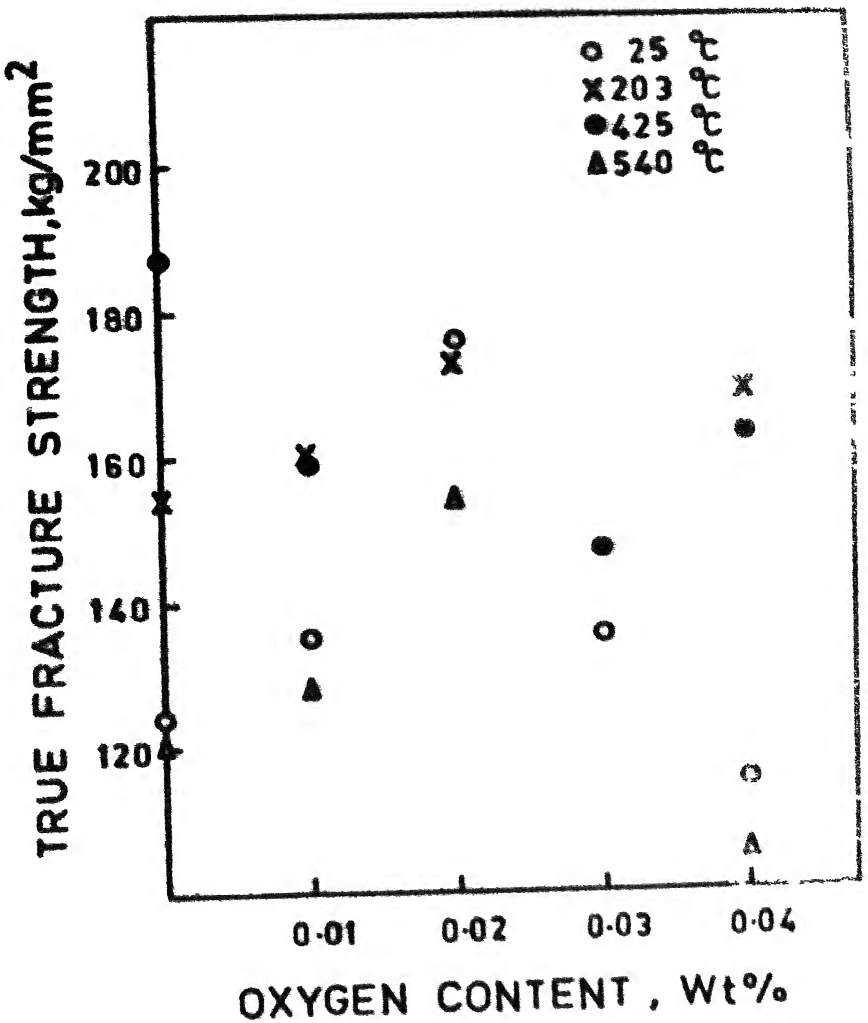

Fig·3·12 True fracture strength vs oxygen content for modified 9Cr-1Mo steel(annealed and normalized) at various temperatures.

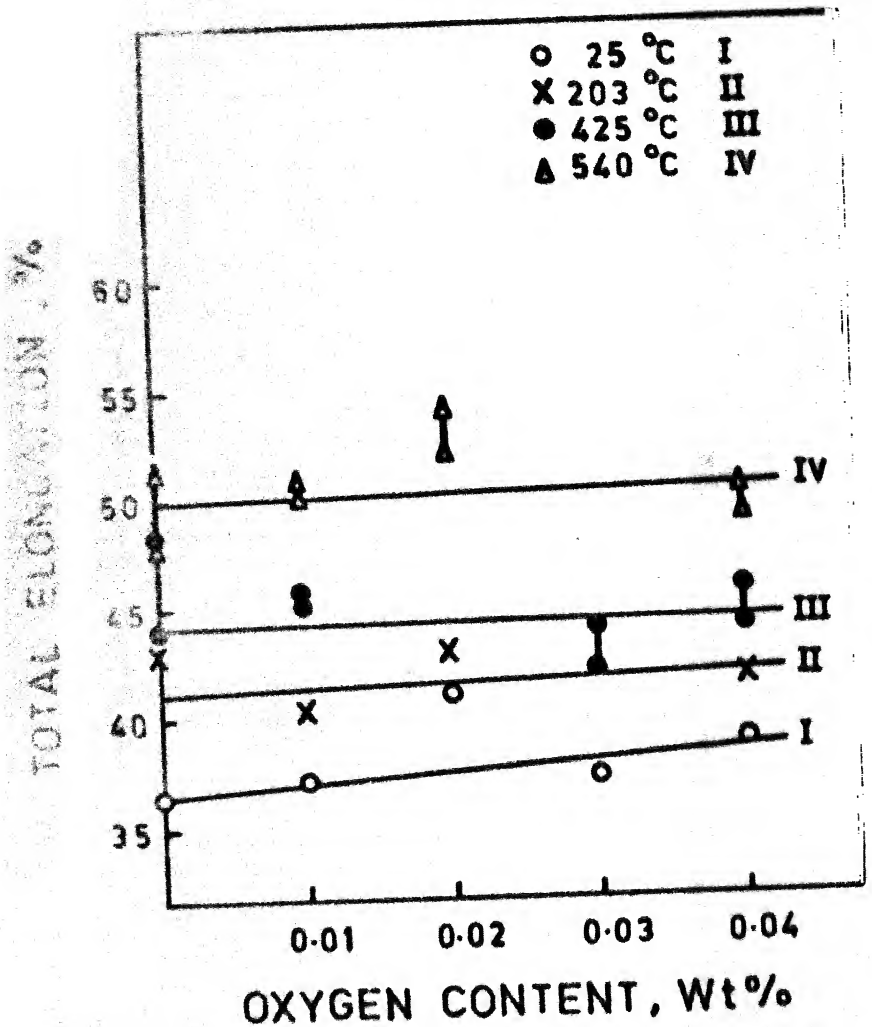

Fig 3·13 Total elongation vs oxygen content for modified 9Cr-1Mo steel(annealed and normalized) at various temperatures.

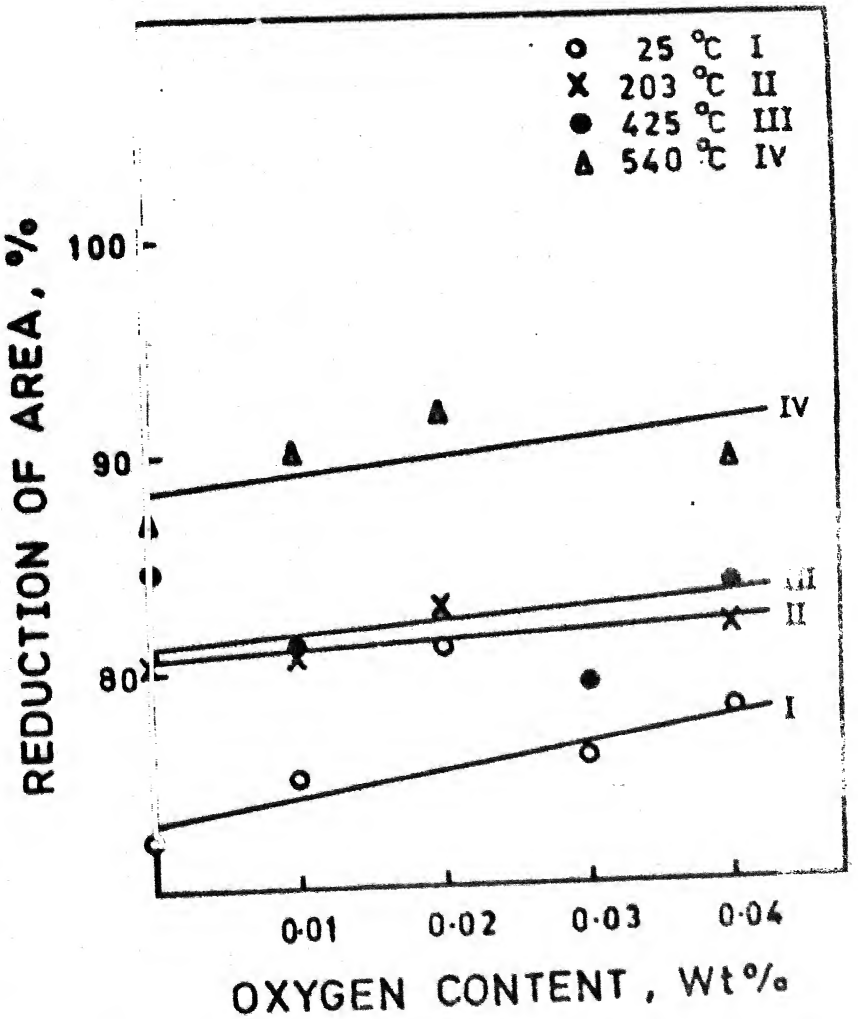

Fig·3·14 Reduction of area vs oxygen content for modified 9Cr-1Mo steel(annealed and normalized) at various temperatures.

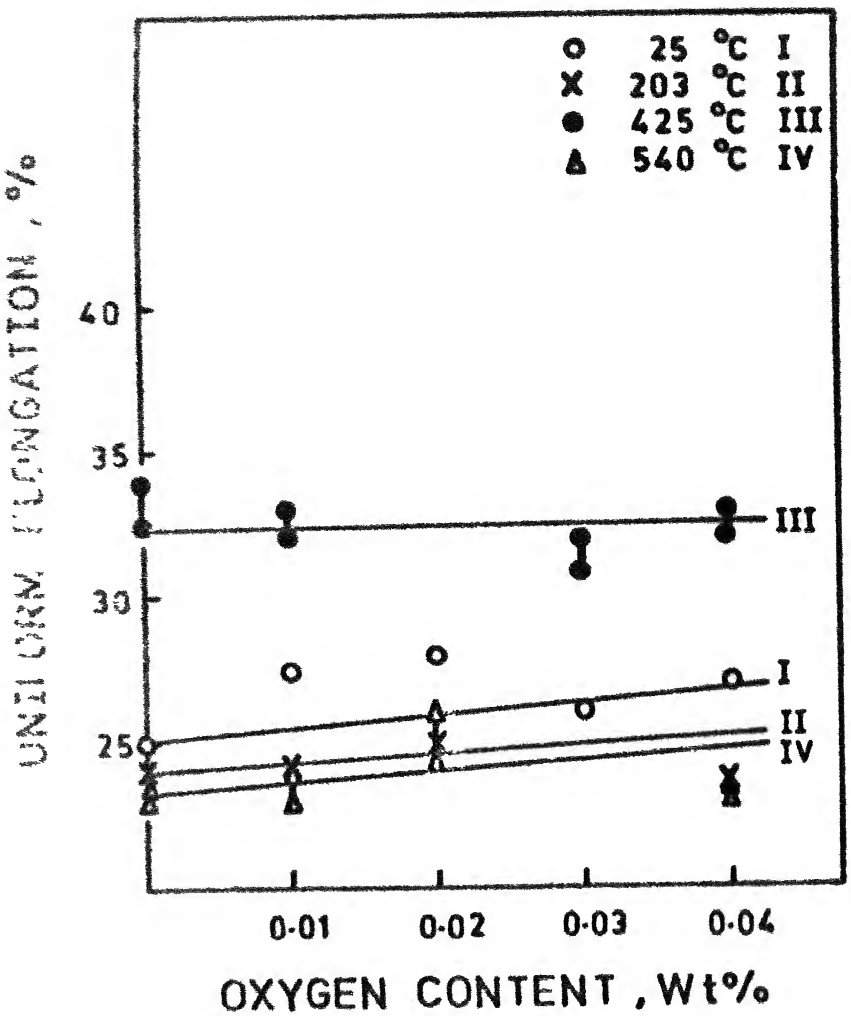

Fig·3·15 Uniform elongation vs oxygen content for modified 9Cr-1Mo steel(annealed and normalized) at various temperatures.

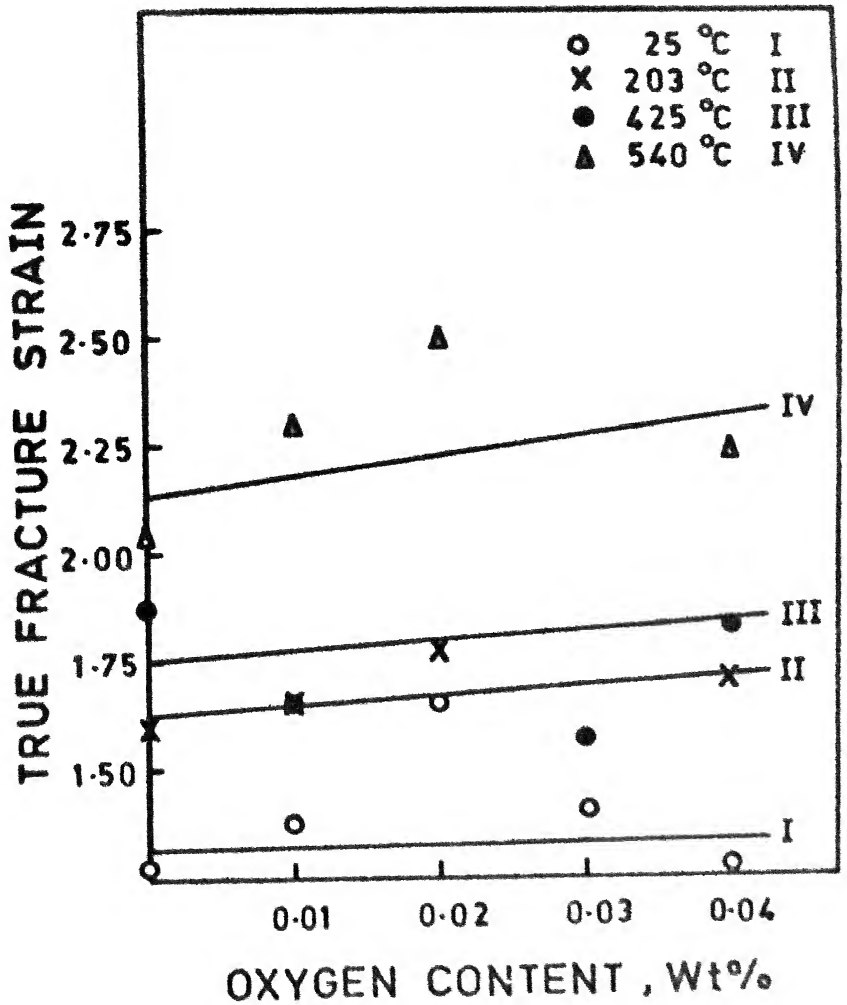

Fig·3·16 True fracture strain vs oxygen content for modified 9Cr-1Mo steel(annealed and normalized) at various temperatures.

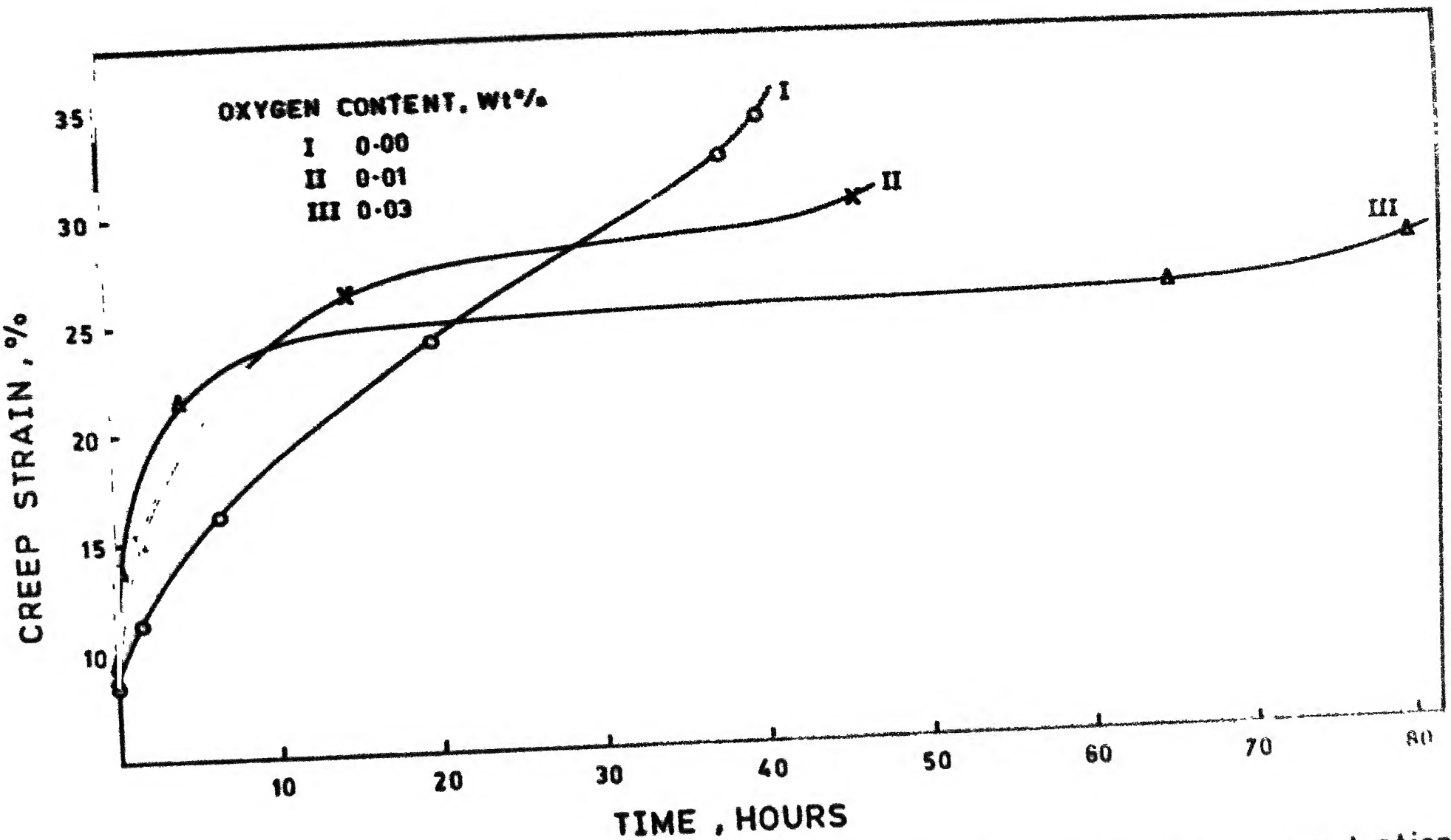

Fig·3·17 Creep curves for modified 9Cr-1Mo steel at various oxygen concentrations.

3.1.4 X-ray Diffraction:

Results of X-ray analysis of normalized and tempered, modified 9Cr-1Mo steels are shown in Table 3.3, for unoxidized tensile tested, oxidized and stress-ruptured samples. With comparison of d values listed in X-ray diffraction data files, MoO_3, $FeCr_2O_4$, Fe_2O_3 compounds were identified in the oxidized stress-ruptured sample in addition to those present in the unoxidized sample. Some of the peaks' intensities in stress ruptured samples are high as compared to their counterparts in the unoxidized tensile tested sample, while others are low. Appendix-B lists the 'd' values for some of important compounds useful for this analysis.

Results of various mechanical test show the scattering at higher temperature.

3.2 Discussion

3.2.1 Tensile Property:

In all mechanical properties, samples of two different treatments were testedi.e.normalized and tempered (1040°C for 1 h, air cooled to room temperature; 760°C for 1 h, air cooled to room temperature), annealed and normalized (850°C for 1 hr, furnace cooled to room temperature; 760°C for 1 h, air cooled to room temperature). On normalizing from 1040°C, austenite will completely transform to

lath martensite (due to sluggish kinetics of transformation) with a high density of transformation dislocation[6]. But on tempering, according to Baker and Nutting[25], the sequence of carbide precipitation is obtained

$$\varepsilon\text{-Carbide} \longrightarrow \text{Cementite} \longrightarrow \left.\begin{matrix}\text{Cementite} \\ + \\ Mo_2C\end{matrix}\right\} \longrightarrow M_{23}C_6 \longrightarrow M_6C$$

Fine dispersion of $M_{23}C_6$ and MC precipitates have been found to have the composition of $(Cr, Fe,V)_{23}(C,N)_6$ and Nb (C,N) respectively in modified 9Cr-1Mo steel[1]. Tempering results into lower dislocation density in the laths of martensite (likely to be ferrite). Fig. 3.18 and 3.19 reveal the microstructure of normalizedand tempered steel. Annealing and normalizing of the steel, in the microstructure (Fig.3.20, 3.21), nearly complete carbides precipitation preferentially along the grain boundaries (as the high energy sites) and almost dislocation free grains of ferrite. These microstructures of two type of steels are responsible for their corresponding strength. Tensile and yield strength of modified 9Cr-1Mo steel are found higher than that of corresponding, steel's strength of Sikka et.al.[1]. The reason for this is the appreciable higher strain rate applied for test as compared to that of others. Oxidation at 650°C, gives the tempering treatment. Heating at 650°C for shorter time in the normalized and tempered steel results in the rearranging of dislocations and slightly more carbide

precipitation but in annealed and normalized steel, slight grain coarsening occurs. So these treatments result into small decrease in the strength (tensile, yield, fracture) at the test temperature with increase of oxidation time. The negligible oxidation of sample occurs even during the testing at 540°C in air. It is evident from Fig.3.22 as well as brownish colour of sample surface that the oxidation is negligible even after test at 540°C.

Mechanical properties are very much dependent on temperature since the mobility of atoms increases rapidly with temperature so diffusion controlled processes can have a very significant effect on high temperature mechanical properties. High temperature will also result, in greater mobility of dislocation by the mechanism of climb and in the increase of equilibrium concentration of vacancies. New deformation, mechanism may also come into play at elevated temperatures. In some metals the slip system changes or additional slip systems are introduced with increase of temperature. Deformation at grain boundaries becomes an added possibility in high temperature deformation of metals. Prolonged exposure at elevated temperature affects metallurgical stability of metals and alloys eg. recrystallization and grain coarsening, overaging[20]. The path of fracture of metals at elevated temperatures follows the grain boundaries then the fracture is intergranular (or inter crystalline) in contrast to the transgranular

(or intracrystalline) mode of fracture commonly observed at ordinary temperature.

In both the normalized and tempered, annealed and normalized samples, strength (tensile, yield, fracture) decreases with increase of temperature due to the ease of dislocation movement. Fig.3.23 and 3.24 depict the ductile trans-granular fracture at room temperature while Fig.3.25 and 3.26 give the mixed mode of fracture (trans-granular-inter-granular) at 540°C. Ductile nature of modified steel is confirmed by void formation as it is evident from Fig.3.27 and 3.28. Variation of total elongation and reduction of area may be explained in the similar way, so as the temperature increases, the strength decreases and ductility increases with respect to oxidation. In case normalized and tempered steel, a drop in ductility at 203°C is noticed which is confirmed by Sikka et.al.[1] investigation. This effect is attributed to C or N, which can diffuse rapidly at 200 to 300°C and react with dislocation as they accumulate within the specimen during the test, and results into pinning effect. Below thistemperature range dislocation remain unpinned because the time of testing is too short to permit an atmosphere of C atoms to collect around dislocation introduced by plastic flow, whereas at higher temperatures the C-atoms are so mobile that they can not act to pin dislocation[22]. But this reason, could not explain satisfactorily because in such case steel should show a peak

strength at this temperature and enough amount of C-atoms is also not available. Minor increase in the uniform elongation with increase of oxidation time at a test temperature is understood clearly as the reason of strength, ductility variation. The change in uniform elongation with temperature could not be understood clearly. It may be due to the activities of alloy elements at respective temperatures or else.

The scattering in the true fracture stress could not be explained. Possibly one of the reasons could be the stress taken should be corrected for the triaxial state of stress existing in the tensile specimen at fracture. Since data required for this correction are not available, true fracture stress values are so frequently in error[20]. Variation of true fracture strain with respect to oxidation and temperature is according to the reduction of area as true fracture strain is derived from the reduction of cross-section area at fracture.

3.2.2 Low Cycle Fatigue Property:

The low cycle fatigue strength or number of cycle to failure decreases with increase of oxygen content in both normalized and tempered, annealed and normalized samples. This may be due to two reasons:

(1) lowering of strength with increase of oxidation time, (2) wedging action of oxide scale as shown in Fig.3.29. Fig.3.30 shows no beach mark on the fracture surface because of rubbing action of two faces.

3.2.3 Creep-fatigue and Creep Properties:

Increase in the cycling strength with oxygen content at 540°C for the normalized and tempered samples is attributed to change in microstructure. Bainitic structure with carbide precipitates has been found best structure for creep resistance[26,27]. With increase of oxidation time, microstructure transforms towards more stable structure (bainitic). Various carbides as Nb, V carbides precipitate with negligible coarsening of tempered carbide and minor change in structure morphology occurs as shown in Fig.3.31.

Fig.3.32 shows dislocation band of fatigue at the gauge region.

Increase in tensile strength and decrease in ductility of annealed and normalized steel after fatigue cycling (Table 9 (Appendix-A)) may be due to strain hardening because of plastic deformation. From optical micrograph and fractograph (Fig.3.33 and 3.34), it can be concluded the mode of fracture is mixed in nature (Intergranular-Transgranular).

Improvement in stress-rupture strength of normalized and tempered steel, with the oxidation time can be explained in similar way as that of creep-fatigue strength of normalized and tempered steel. Fig.3.35 shows the microstructure of stress-ruptured specimen. Further this figure shows no intergranular creep cavitation occurs in this steel so the decrease in rupture strain with time can be attributed to segregation of impurities to grain boundaries in long term which reduces interfacial energy[28]. Fig.3.36 shows a glimps of impurity segregation. Stress rupture sample shows mixed mode of fracture as shown in Figs.3.37 and 3.38.

It is evident from Fig.3.39 and 3.40 that void density in creep fatigue and stress-ruptured samples are higher than that of simple tensile tested samples (Fig.3.27 and 3.28). This excessive voids formation may be due to extra precipitation as evidenced by the appearance of extra height of peaks in X-ray diffraction of stress-ruptured samples compared with simple tensile tested sample and microhardness (Table 11 (Appendix-A)).

Scattering in mechanical property may originate from two sources: test parameter variability and metallurgical variability[29]. Test variable may be stress and temperature, sample surface finish, dimension etc. and metallurgical variable may be compositional, microstructural.

Figure 3.41 shows one of the various defects in the present work.

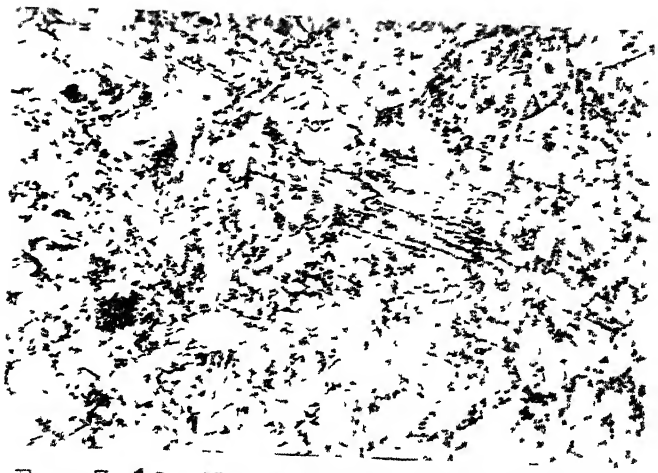

Fig.3.18: Normalized and Tempered Sample, X 600

Fig.3.19: Normalized and tempered sample, tensile tested at 25°C, X 1200

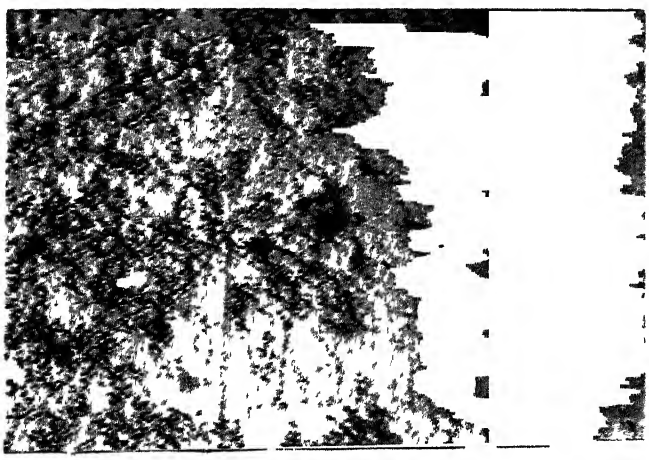

Fig.3.20: Annealed and normalized sample, X 00

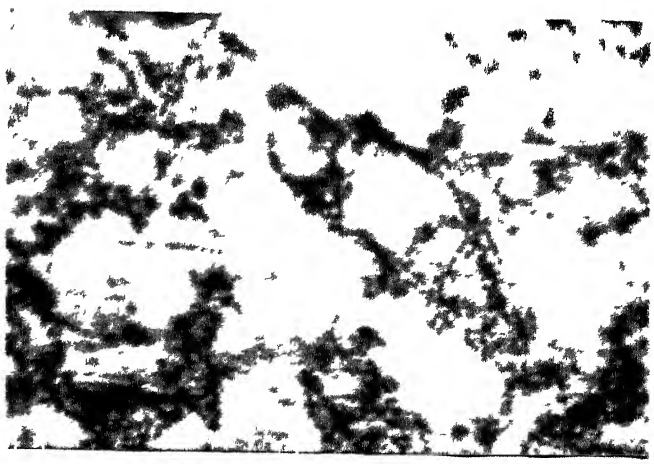

Fig.3.21: Annealed and normalized sample, X 1200

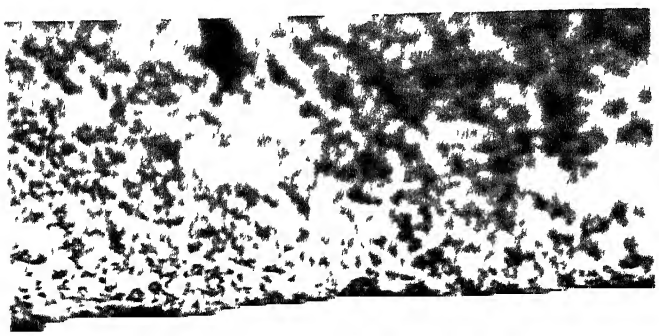

Fig.3.22: Cross-section of sample, tensile tested at 540°C, X 600

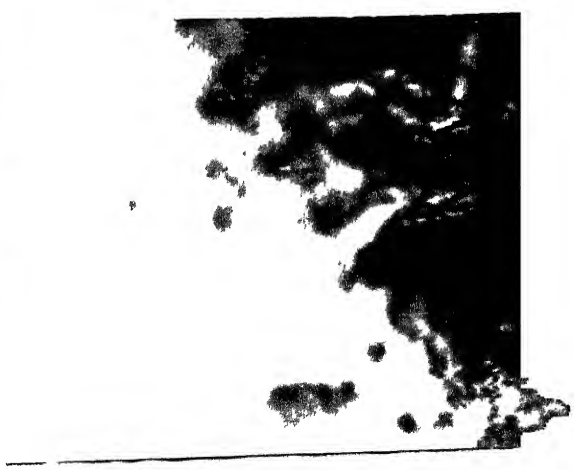

Fig.3.23: Fracture edge of normalized and tempered sample, tensile tested at 25°C, X 1200

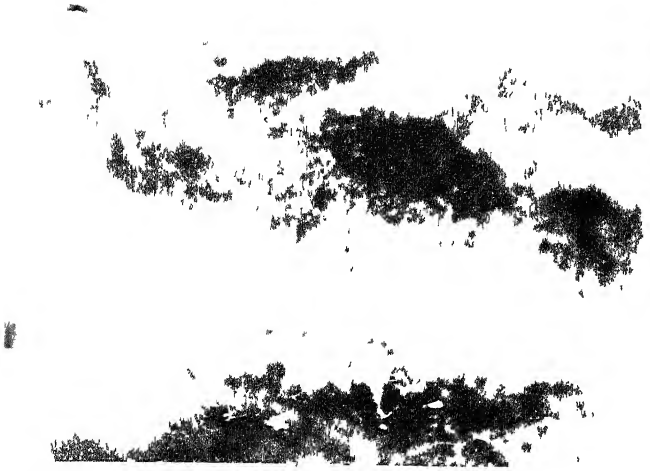

Fig.3.24: Fracture edge of annealed and normalized sample, tensile tested at 25°C, X 1200

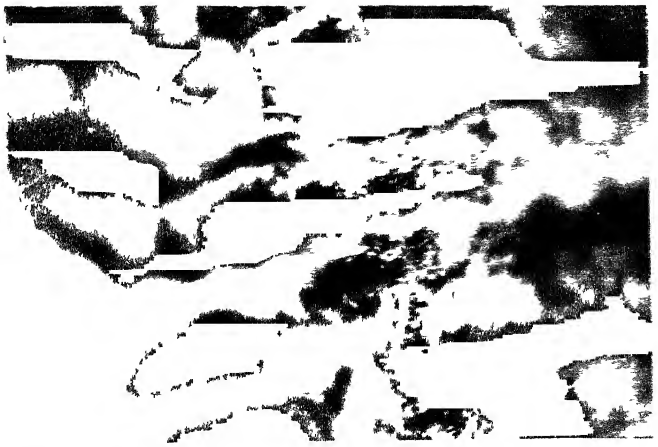

Fig.3.25 : Fracture edge of normalized and tempered sample, tensile tested at 540°C, X 1200

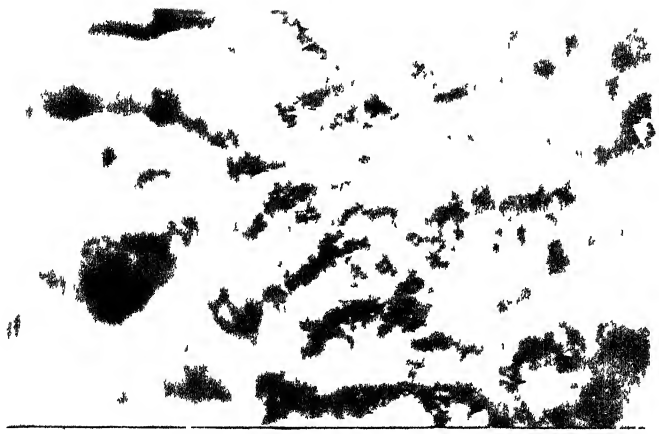

Fig.3.26: Fracture edge of annealed and normalized sample, tensile tested at 540°C, X 1200

Fig.3.27: Normalized and tempered sample, tensile tested at 25°C, X 500

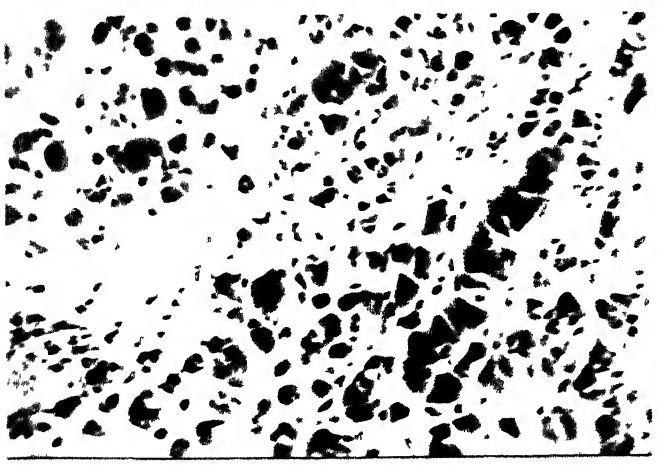

Fig.3.28: Normalized and tempered sample, tensile tested at 25°C, X 1000

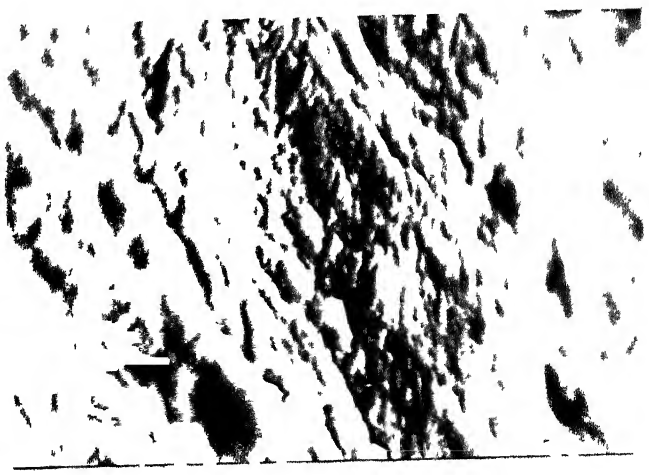

Fig.3.29: Oxide scale on the fatigued sample, X 1000

Fig.3.30: Fracture surface of the fatigued sample, X 300

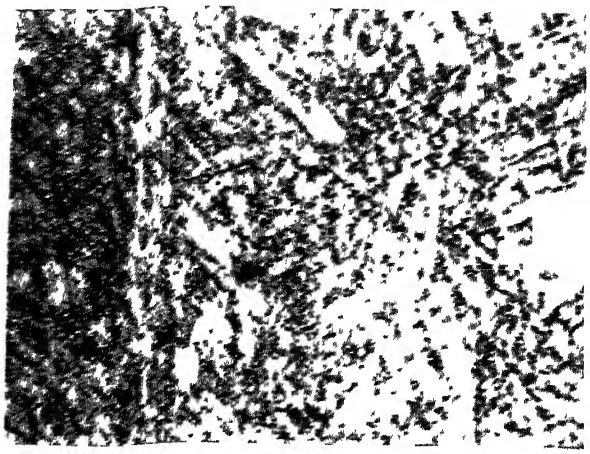

Fig.3.31: Normalized and tempered sample, fatigued at 540°C, X 1200

Fig.3.32: Gauge region of normalized and tempered sample, fatigued at 540°C, X 1200

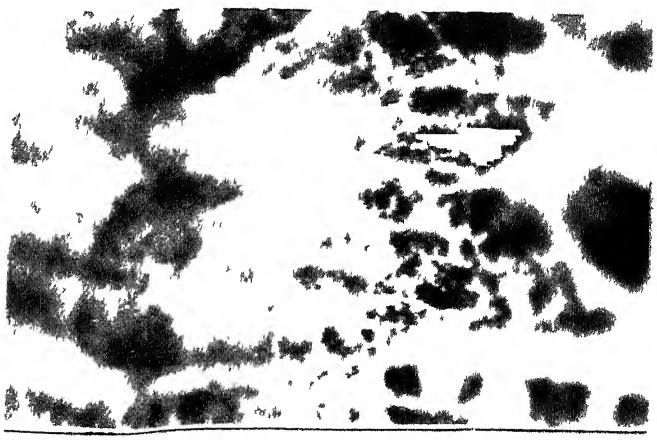

Fig.3.33 : Fracture edge of annealed and normalized sample, fatigued and tensile tested at 540°C, X 1200

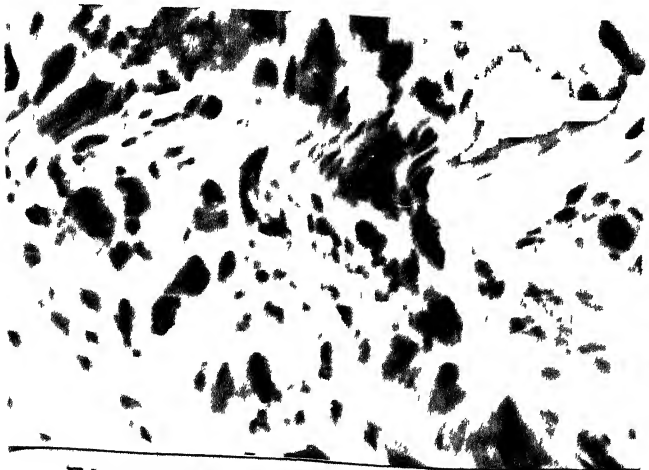

Fig.3.34: Annealed and normalized sample fatigued and tensile tested at 540°C, X 1500

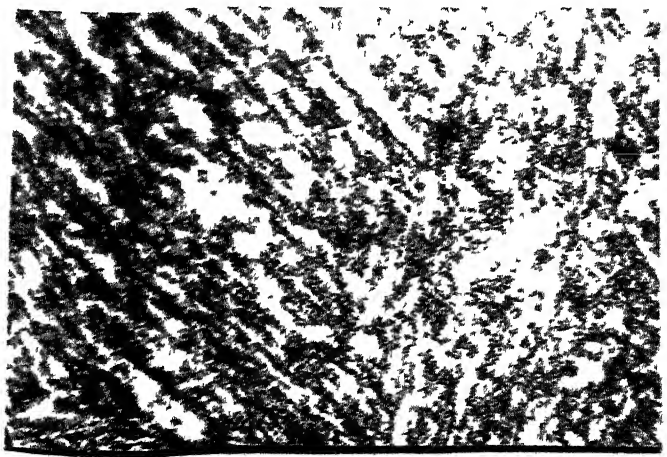

Fig.3.35: Normalized and tempered sample, stress-ruptured at 540°C, X 1200

Fig.3.36: Normalized and tempered sample, stress-ruptured at 540°C, X 2100

Fig.3.37: Fracture edge of stress-ruptured sample at 540°C, X 1200

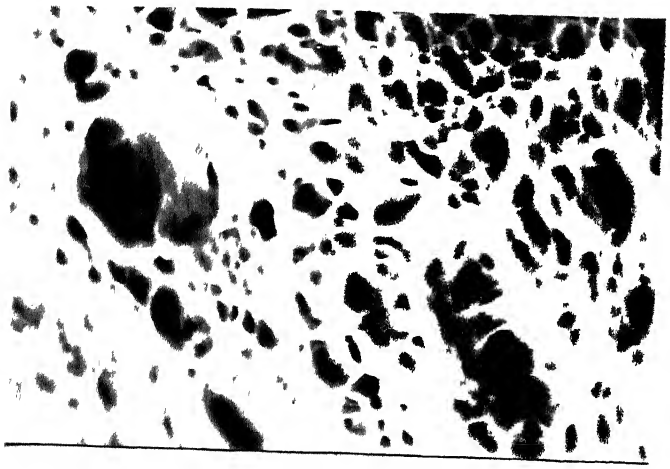

Fig.3.38: Stress-rupture sample at 540°C, X 1500

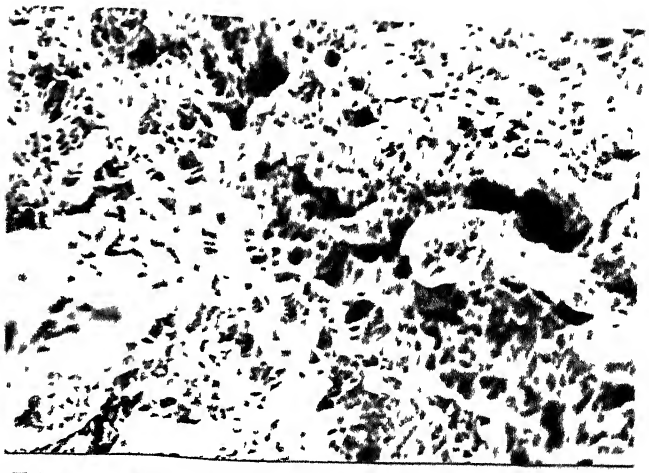

Fig.3.39: Normalized and tempered sample, fatigued at 540°C, X 250

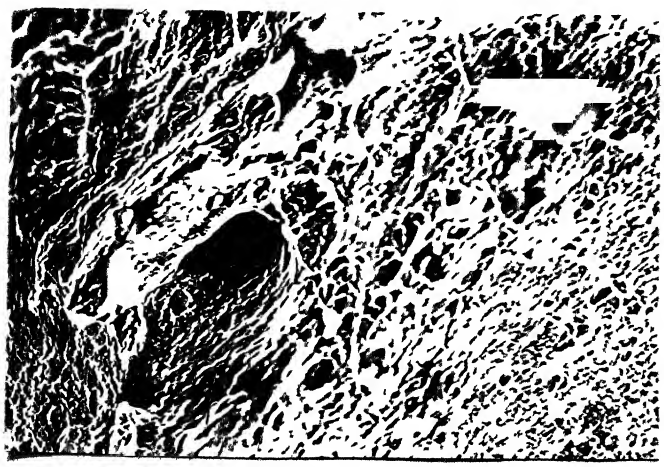

Fig.3.40: Normalized and tempered sample, stress-ruptured at 540°C, X 250

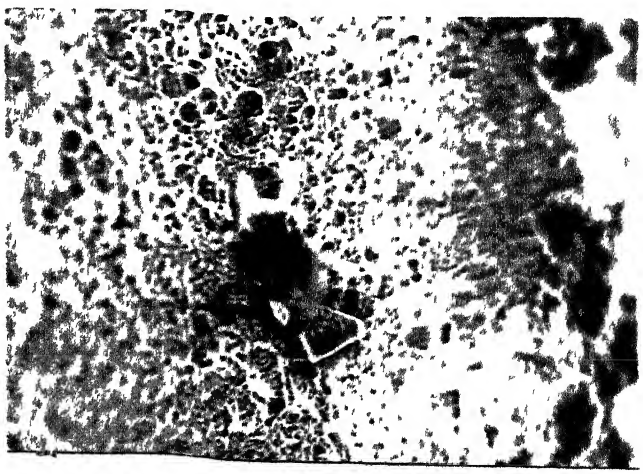

Fig.3.41: Normalized and tempered sample, tensile tested at 540°C, X 250

CHAPTER 4

CONCLUSIONS

The conclusionson the study of effect of oxidation on Mechanical Behaviour of Modified 9Cr-1Mo ferritic steels are summarised below.

1. The oxide scale made at 650°C consists of molybdenum oxide, iron-chrome spinel and iron oxide in outer layer.

2. The slight decrease in strength (tensile, Yield, fracture, at the test temperature with increase of oxidation time is attributed to the microstructural changes.

3. The strength of this steel (normalized and tempered, annealed and normalized) decreases with increase of temperature.

4. The ductility of modified 9Cr-1Mo steel is observed increasing with the temperature but drops at 203°C for normalized and tempered condition.

5. The fatigue strength is decreased with increase of oxygen content in both normalized and tempered, annealed and normalized conditions. It is attributed to the wedging action of oxides and the microstructure of steel.

6. The creep-fatigue strength and creep strength is found to be improved with increase of oxidation time under normalized and tempered condition of this steel. This is due to the precipitation of carbides and stabilized structure

probably of bainitic nature.

7. The fractography, X-ray diffraction studies revealed the higher density of voids in stress-ruptured sample compared to the tensile tested sample which is an evidence of precipitation in the matrix during creep.

8. The tensile strength at 540°C after the cycling at same temperature is observed to increase under annealed and normalized condition. It may be due to the strain hardening resulting from plastic deformation.

probably of bainitic nature.

7. The fractography, X-ray diffraction studies revealed the higher density of voids in stress-ruptured sample compared to the tensile tested sample which is an evidence of precipitation in the matrix during creep.

8. The tensile strength at 540°C after the cycling at same temperature is observed to increase under annealed and normalized condition. It may be due to the strain hardening resulting from plastic deformation.

CHAPTER 5

NEED OF FUTURE WORK

Present work is a preliminary attempt towards the understanding of effect of oxidation on mechanical behaviour of modified 9Cr-1Mo steel. However, a large number of querries are still unsolved. Hence a further work is needed to understand the alloy behaviour more clearly. Some of these are worth mentioning here.

1. To study the effect of oxidation on the mechanical behaviour at the higher temperature for the longer duration of time.

2. The scattering in data of true fracture stress and other related mechanical properties need a detailed investigation.

REFERENCES

1. V.K.SIKKA et.al., Modified 9Cr-1Mo steel an improved alloy for steam generator application. Conf. Proc. Ferritic steels for High Temperature Applications, ASM-6-8 Oct. 1981, pp.65.

2. V.K.SIKKA, "Substitution of modified 9Cr-1Mo steel for austenitic stainless steel", ORNL-5841, April 1982.

3. CUNNIGHAM et.al., Ferritic steels as alternate structural materials for high temperature application, Edited by Ashok K.Khare, ASM, pp.3-6.

4. M.K.BOOKER et.al., Comparison of mechanical strength properties of several high-chromium-ferritic steels, ibid, pp.257-273.

5. SADAHIKO MURASE et.al., The properties of modified 9% Cr-1% Mo steel, Tenpaloy F-9, Int. Conf. on Production fabrication, properties and application of ferritic steels for high temperature application, ASM, 6-8 Oct.1981, pp.116-130.

6. WENDELL B.JONES, Effect of mechanical cycling on the structure of modified 9Cr-1Mo ferritic steels, ibid., pp.221-220.

7. R.T.KING and L.EGNELL, "Historical development of steels containing 8-10% Cr and 0-2% Mo and future directions for LMFBR applications", Int. Conf. Ferritic Steels for Fast Reactor Steam Generators, 30 May - 2 June 1977, BNES, London, pp.74-81.

8. K.P.SINGH and K.BATRA, Study of mechanical and oxidation behaviour of chromium-molybdenum ferritic steel in various atmosphere - Technical Report, No.3, D.A.E., Govt. of India, pp. 28, 61.

9. DORN et.al., Materials at high temperature, pp.85-90.

10. WILLBY and WALSER, 'Material choice for the commercial fast reactor steam generators', Int. Conf. Ferritic Steels for Fast Reactor Steam Generators, 30 May - 2 June, 1977, BNES. London, pp.40-49.

11. KUBASCHEWSKI et.al., Oxidation of metals and alloys, pp. 108-113, 230-240.

12. LAWRENCE AROKIADASS, M.Tech. Thesis, Study of Oxidation and mechanical behaviour of Cr-Mo ferritic steels, I.I.T.-Kanpur (1982).

13. N.BIRKS et.al., Introduction of high temperature oxidation of metals, p.110.

14. FINNIE et.al., Creep of engineering materials.

15. D.CAPLAN, et.al., Corrosion Science, Vol. 10, 1970, pp.1-8.

16. PILLING and BEDWORTH, Journal of institute of metals, Vol. 29 (1923), pp.529-591.

17. O.A.TASCHE, Transactions, American Society for Metals, Vol.42 (1950), p.641.

18. D.CAPLAN, G.I.SROULS and R.J.HUSSEY, Corrosion Science, Vol. 10 (1970), pp.9-17.

19. S.K.VARMA, Oxidation/sulfidation behaviour of some ferritic stainless steels in high temperature coal gasification atmospheres. Int. Conf. Proc. ASM,6-8, Oct. 1981.

20. GEORGE, E.DIETER, Mechanical Metallurgy, pp.331-400.

21. G.V.SMITH, Properties of metals at elevated temperatures, pp.20-53.

22. F.R.SHANLEY, et.al., Mechanical behaviour of materials at elevated temperatures, pp.79-103.

23. K.R.WILLIAMS, et.al., The effect of secondary precipitation on the creep strength of 9Cr-1Mo steel, Int. Conf. Proc.-creep and fracture of Engg. Materials and Structures, 24th - 27th March, 1981, pp.475-485.

24. S.J.SANDERSON, Mechanical properties and metallurgy of 9% Cr-1% Mo steel. ASM Int.Conf. Proc. 6-8 Oct. 1981, pp.92-94.

25. R.G.BAKER and J.NUTTING, Journal of Iron and steel institute, London, Vol. 192 (1959), p.257.

26. CHAKRAVARTY, et.al., Heat treatment of creep resistant steel, Tool & Alloy Steels - April 1978, Vol. 12, No.1, p.111.

27. SOKOLYANSK, The influence of regime of heat treatment and the type of structure of Cr-Mo-V steels on the thermocycle strengths: Ist international congrees on Heat Treatment of Material (Proc. Conf.) Warsaw, 27-30 Oct. 1981.

28. POPE, et.al., Grain boundary impurity effects on the creep ductility of ferritic-steels, Int. Conf. Proc. on creep and fracture of engg. materials and structures, 24-27 March, 1981, pp.531-41.

29. BRESSERS, et.al., Analysis of the causes of scatter in stress-rupture properties of a Ni-base alloy, ibid, pp.461-62.

30. Fractography and Atlas of fractographs, Metals Handbook. ASTM, Vol.9.

TABLE 2 : The results of tensile tests at 203°C for normalized and tempered steel

wt.%	UTS kg/mm^2	0.2% offset yield strength kg/mm^2	Engg. fracture strength kg/mm^2	True fracture strength kg/mm^2	Total elongation %	Uniform elongation %	Reduction of area, % 'q'	True fracture strain ln (1/1-q)
0.00	74.43	54.2	51.98	162.43	18.0	13.1	68.0	1.139
0.01	72.33	52.0	51.03	146.63	18.8	13.0	65.2	1.05
0.02	68.15	52.8	50.17	145.84	21.5	15.0	65.6	1.06
0.04	68.95	50.0	50.32	162.32	21.7	14.0	69.0	1.17

TABLE 3 : The results of tensile tests at 425°C for normalized and tempered steel

Oxygen content wt. %	UTS kg/mm^2	0.2%offset yield strength kg/mm^2	Engg. fracture strength kg/mm^2	True fracture strength kg/mm^2	Total elonga-tion %	Uniform elonga-tion %	Reduction of area, % 'q'	True fracture strain ln (1/1-q)
0.00	60.71	50.0	44.64	182.95	30.5	19.3	75.6	1410
	68.09		47.71		28.0	17.0		
0.01	65.13	49.2	45.98	170.29	29.1	18.2	73.0	1.31
	71.02		54.20		25.0	15.5		
0.03	62.57	45.2	45.12	155.58	29.7	18.0	71.0	1.23
	69.29		52.21		27.2	16.2		
0.04	60.21	45.0	43.93	170.27	31.2	19.0	71.2	1.26
	59.65		43.03		32.0	21.1		

TABLE 4 : The results of tensile tests at 540°C for normalized and tempered steel

Oxygen content wt. %	UTS kg/mm^2	0.2%offset yield strength kg/mm^2	Engg. fracture strength kg/mm^2	True fracture strength kg/mm^2	Total elonga-tion %	Uniform elonga-tion %	Reduction of area, % 'q'	True fracture strain ln (1/1-q)
0.00	53.03	40.02	25.25	135.02	37.2	17.0	81.3	1.67
	50.15		23.84		38.1	17.8		
0.01	55.63	41.35	30.07	189.12	36.0	16.8	84.1	1.83
	52.16		25.23		37.0	17.6		
0.02	46.68	37.0	24.27	142.76	38.0	18.0	83.0	1.77
	57.36		34.88		33.5	16.0		
0.04	50.83	38.0	24.90	128.35	37.8	17.8	80.6	1.69
	49.63		23.38		39.0	18.4		

TABLE 5 : The results of tensile tests at 25°C for annealed and normalized steel

Oxygen content wt. %	UTS kg/mm^2	0.2% offset yield strength kg/mm^2	Engg. fracture strength kg/mm^2	True fracture strength kg/mm^2	Total elongation %	Uniform elongation %	Reduction of area, % 'q'	True fracture strain ln (1/1-q)
0.00	54	32.0	34.48	124.02	36.3	25.0	72.2	1.28
0.01	53.8	30.8	33.73	134.92	37.2	27.5	75.0	1.386
0.02	52	29.9	33.1	176.06	41.0	28.3	81.2	1.67
0.03	53	31.1	32.72	135.20	37.0	26.0	75.8	1.1189
0.04	52	30.0	32.15	114.8	38.6	27.0	78	1.27

TABLE 6 : The results of tensile tests at 203°C for annealed and normalized steel

Oxygen content wt. %	UTS kg/mm^2	0.2% offset yield strength kg/mm^2	Engg. fracture strength kg/mm^2	True fracture strength kg/mm^2	Total elongation %	Uniform elongation %	Reduction of area, % 'q'	True fracture strain ln (1/1-q)
0.00	50	28.0	30.32	153.90	43.0	24.1	80.3	1.62
0.01	52.1	28.2	30.8	160.41	40.2	24.0	80.8	1.65
0.02	47.35	26.5	29.12	173.33	43.0	25.0	83.2	1.78
0.04	51.1	27.0	30.4	168.88	41.7	23.4	82.0	1.71

TABLE 7 : The results of tensile tests at 425°C for annealed and normalized steel.

Oxygen content wt.%	UTS kg/mm^2	0.2% offset yield strength kg/mm^2	Engg. fracture strength kg/mm^2	True fracture strength kg/mm^2	Total elongation %	Uniform elongation %	Reduction of area, % 'q'	True fracture strain ln (1/1-q)
0.00	41.28	25.3	28.66	187.32	48.2	34	84.7	1.87
	48.56		31.609		44.1	32.5		
0.01	43.31	25.0	30.29	159.42	45.0	33.0	81.0	1.660
	40.21		26.39		45.8	32.2		
0.03	45.02	26.2	30.5	147.34	44.0	32.0	79.3	1.57
	48.30		33.146		42.0	30.7		
0.04	40.01	24.6	26.23	162.92	45.6	32.8	83.9	1.83
	43.11		29.34		44.0	32.0		

TABLE 8 : The results of tensile tests at 540°C for annealed and normalized steel

Oxygen content wt. %	UTS kg/mm^2	0.2% offset yield strength kg/mm^2	Engg. fracture strength kg/mm^2	True fracture strength kg/mm^2	Total elongation %	Uniform elongation %	Reduction of area, % 'q'	True fracture strain ln (1/1-q)
0.00	32.57	19.2	15.7	120.76	51.2	23.4	87.0	2.04
	38.12		18.31		48	23.7		
0.01	31.11	19.0	12.77	127.7	50.0	23.0	90.0	2.3
	30.19		12.27		51.0	24.0		
0.02	29.23	17.0	12.31	153.87	54.0	26.0	92.0	2.52
	30.58		13.02		52.0	24.4		
0.04	29.03	17.3	11.2	104.6	50.1	23.0	89.3	2.23
	32.93		13.85		49.0	23.5		

TABLE 9 : Results of tensile test at 540°C, after creep-fatigue performed on modified 9Cr-1Mo steel (annealed and normalized)

Details of sample	UTS Kg/mm^2	Total elongation, %
0.02% oxygen-creep-fatigue for 9.25 hr. (10^4 cycle with max. stress 27.4 kg/mm^2, than tensile test	34.02	46.09
0.04% oxygen-creep-fatigue for 10.5 hr, (10^4 cycle with max. stress 28.8 kg/mm^2) than tensile test	36.02	43
0.04% oxygen-creep-fatigue for 11 hrs. (5000 cycle with max. stress 27.4 kg/mm^2 , 5000 cycle with max. stress 30kg/mm^2, 5000 cycle with max.stress 32kg/mm^2) than tensile test	39.82	39

Table 10 : Stress-rupture (at 540°C) data for modified 9Cr-1Mo steel (normalized and tempered)

Specimen with oxygen 0.00%		Specimen with oxygen 0.01%		Specimen with oxygen 0.02%		Specimen with oxygen 0.03%	
Time 'hr'	Strain %	Time 'hr'	Strain %	Time 'hr'	Strain %	Time 'hr'	Strain %
0.0	8.5	0.0	8.9	0.0	9.2	0.0	9.6
1.4	11.3	1.2	15.1	1.0	Failed due to jerk	0.4	13.8
6.6	16.2	15.0	26.3	-	-	4.4	21.5
20.0	24.0	46.0	30 Failure	-	-	64.9	25.7
38.0	32.2	-	-	-	-	79.8	27.8 Failure
40.2	34 Failure	-	-	-	-	-	-

Table 10 : Stress-rupture (at 540°C) data for modified 9Cr-1Mo steel (normalized and tempered)

Specimen with oxygen 0.00%		Specimen with oxygen 0.01%		Specimen with oxygen 0.02%		Specimen with oxygen 0.03%	
Time 'hr'	Strain %	Time 'hr'	Strain %	Time 'hr'	Strain %	Time 'hr'	Strain %
0.0	8.5	0.0	8.9	0.0	9.2	0.0	9.6
1.4	11.3	1.2	15.1	1.0	Failed due to jerk	0.4	13.8
6.6	16.2	15.0	26.3	-	-	4.4	21.5
20.0	24.0	46.0	30 Failure	-	-	64.9	25.7
38.0	32.2	-	-	-	-	79.8	27.8 Failure
40.2	34 Failure	-	-	-	-	-	-

TABLE 11 : Results of the microhardness test, performed on sample tested for various conditions, at room temperature using Vicker Pyramid-indentor of 136° phase to phase angle

Details of the sample	[illegible]
Annealed and normalized, sample tensile tested at room temperature (No oxidation)	197.1
Annealed and normalized, sample tensile tested at 540°C (oxidized for 1½ hr)	201.88
Annealed and normalized, sample creep fatigued and tensile tested at 540°C (oxidized for 1½ hr)	260.98
Normalized and tempered, sample tensile tested at room temperature (No oxidation)	278.78
Normalized and tempered, sample stress-ruptured at 540°C (oxidized for 1½ hr)	260.98
Normalized and tempered, sample stress-ruptured at 540°C (No oxidation)	269.2
Normalized and tempered, sample creep fatigued at 540°C (oxidized for ½ hr)	275.83
Normalized and tempered, sample creep fatigued at 540°C (oxidized for 1 hr)	283.8

APPENDIX-B

X-ray Diffraction Data for some important compounds

Compound	'd' values			I/I_1 ratio			Card No.
$-Fe_2O_3$	2.69	1.69	2.51	100	60	50	13-534
$-Fe_2O_3$	2.52	2.95	1.61	101	101	101	15-615
Fe_3O_4	2.53	1.61	1.48	100	85	85	11-614
FeO	2.15	2.49	1.52	100	80	60	6-615
$-Fe_2O_3.H_2O$	4.21	2.69	2.44	100	80	70	38-97
$FeCr_2O_4$	2.51	1.91	1.61	100	75	75	4-759
$FeMoO_4$	2.88	1.68	3.56	100	70	40	16-326
MoO_2	3.41	2.42	1.70	100	85	80	5-0452
MoO_3	3.26	3.81	3.46	100	82	61	5-508
$(Cr,Fe)_2O_3$	1.68	3.68	2.69	100	80	80	2-1357
Cr_2N	2.10	2.38	2.22	100	25	25	1-1232
CrN	2.07	2.39	1.46	100	80	80	11-65
Cr_2O_3	2.67	2.48	1.67	100	96	90	6-504
CrO_2	3.11	1.63	2.42	100	75	60	9-332
CrO_3	4.16	3.42	3.36	100	100	100	9-47